

## $\pi N$ Scattering in the $\Delta(1232)$ Region in an Effective Field Theory

Bingwei Long<sup>1,2,\*</sup> and U. van Kolck<sup>2,†</sup>

<sup>1</sup>*European Centre for Theoretical Studies in Nuclear Physics and Related Areas (ECT\*),*

*Strada delle Tabarelle 286, I-38100 Villazzano (TN), Italy*

<sup>2</sup>*Department of Physics, University of Arizona,*

*1118 East 4th Street, Tucson, Arizona 85721, USA*

(Dated: October 25, 2018)

### Abstract

We develop a generalized version of heavy-baryon chiral perturbation theory to describe pion-nucleon scattering in a kinematic domain that extends continuously from threshold to the delta-isobar peak. The  $P$ -wave phase shifts are used to illustrate this framework. We also compare our approach with those in the literature that concern the delta resonance.

Keywords: chiral perturbation theory; pion-nucleon scattering; delta-isobar resonance

arXiv:0907.4569v2 [hep-ph] 10 Apr 2010

---

\*Corresponding author. Tel: +39(0461)314-776; Fax: +39(0461)935-007; Email: long@ect.it

†Email: vankolck@physics.arizona.edu

## I. INTRODUCTION

Pion exchange provides the long-range components of nuclear forces, and crucial to its understanding is pion-nucleon ( $\pi N$ ) scattering. A prominent feature of the latter is the delta resonance,  $\Delta(1232)$ , a peak in the elastic cross section at the center-of-mass (CM) energy  $m_\Delta \equiv m_N + \delta \simeq 1230$  MeV, where  $\delta \sim 290$  MeV is the nucleon-delta mass splitting [1]. Our goal here is to investigate  $\pi N$  scattering from threshold up to the delta resonance in an effective field theory (EFT).

It is well known that resonances can be studied by considering the unitarity and analyticity of the  $S$  matrix. Assuming for simplicity that there is only one decay channel for a resonance, when the CM energy  $E$  is close enough to the resonance, the  $T$ -matrix element in the resonance channel can be written in the form of a Breit-Wigner formula plus a non-resonant background (see, *e.g.*, Refs. [2, 3]),

$$T(E) \equiv -i \{ \exp [2i\theta(E)] - 1 \} = -\frac{\Gamma}{E - E_R + i\Gamma/2} (1 + iT_B) + T_B, \quad (1)$$

where  $\theta(E)$  is the phase shift,  $E_R$  and  $\Gamma/2$  are real numbers that represent the energy and half-width of the resonance (that is, the pole position in the complex-energy plane), and  $T_B$  is a complex number often called the non-resonant background amplitude, which can be written as  $T_B = -i[\exp(2i\theta_0) - 1]$  in terms of a non-resonant phase shift  $\theta_0$ .

Though based on general principles, the direct application of Eq. (1) relies on a few assumptions. First, in many cases where  $E_R$  and  $\Gamma$  are unknown *a priori*, they are free parameters of Eq. (1) despite the fact that they are related in some underlying theory (which is Quantum Chromodynamics (QCD) in the delta case). In the absence of  $T_B$ , one could precisely determine  $E_R$  by where the phase shift passes through  $\pi/2$  (hence a sharp peak in the cross section). However,  $T_B$  is in general non-vanishing so one has to make an educated guess about where the resonance window is centered. Therefore, the values of  $E_R$ ,  $\Gamma$ , and  $T_B$  based on Eq. (1) may be model-dependent. Second, one has to assume how close to the resonance is “close enough”. Particularly, is  $E_R$  small enough so that Eq. (1) is valid even at threshold? If Eq. (1) works only in the resonance region, one has to assume that the data points one wants to fit are sufficiently close to the resonance. Or can we extend Eq. (1) simply by allowing  $T_B$  and/or  $\Gamma$  to be functions of energy (as it happens in general in field theory) and, if so, with what constraints on  $T_B(E)$  and  $\Gamma(E)$ ? If  $\Gamma$  depends on the energy, then the position of the pole is *not* given by  $E_R - i\Gamma(E_R)/2$ , and the physical interpretations of  $E_R$  and  $\Gamma(E_R)$  are unclear. In the case of the delta, one can show explicitly [4] that  $E_R$  and  $\Gamma(E_R)$  are indeed unphysical in the sense that they depend at two-loop level on the choice of fields.

Given that one cannot, at present, straightforwardly solve QCD at low energies due to the difficulties posed by the large strong-coupling constant and the small pion mass  $m_\pi$ , EFT is a good alternative for describing low-energy nuclear and hadronic physics consistently. Following several seminal papers [5], EFTs have been developed as model-independent approximations to low-energy strong interactions, which can be systematically improved by a series in powers of  $Q/M_{\text{QCD}}$ , where  $Q$  refers generically to small external momenta and  $M_{\text{QCD}} \sim 1$  GeV is the characteristic QCD scale. The loyalty of EFTs to QCD, the underlying theory of low-energy strong interactions, is manifested by the fact that EFTs inherit all the symmetries of QCD, among which chiral symmetry is probably the most nontrivial. For reviews, see, for example, Refs. [6, 7].

A particular EFT, chiral perturbation theory (ChPT), specializes, and has proven quite successful, in processes involving at most one nucleon [6]. At energies  $E$  close to the  $\pi N$  threshold,  $E \sim m_\pi$ , that is, for  $Q$  around the pion mass, the delta dynamics can be considered short-range physics, which amounts to treating  $\delta$  as a large scale,  $Q \sim m_\pi \ll \delta$ . ChPT with only pion and nucleon fields has been extensively applied to  $\pi N$  scattering near threshold [8–11]. However, it is a perturbative expansion in powers of  $Q/\delta$  and  $m_\pi/\delta$ , which should converge slowly because in the real world  $\delta \simeq 2m_\pi$ . The slow convergence then contaminates pion-exchange nuclear forces [12], where pion energies  $\omega$  are small compared to the  $\pi N$  threshold energy,  $\omega \ll m_\pi$ .

One can improve convergence by considering the delta as an explicit degree of freedom, in which case one can take  $Q \sim m_\pi \sim \delta$ . One can show that hadronic scattering amplitudes can be written as perturbative series in powers of  $Q/M_{\text{QCD}}$ ,  $m_\pi/M_{\text{QCD}}$ , and  $\delta/M_{\text{QCD}}$  [13, 14], and that pion-exchange nuclear forces display a good convergence pattern [12, 15, 16]. The positive role of an explicit delta field in  $\pi N$  scattering within ChPT has been explored [17] and demonstrated in a fully consistent calculation [18].

Nevertheless, this perturbative expansion diverges around the resonance, where the delta goes on-shell. This is not surprising since the perturbative nature of standard ChPT makes it impossible to describe such a non-perturbative phenomenon. In order to fully describe low-energy  $\pi N$  scattering one needs to resum certain terms in the expansion so as to have finite results throughout the low-energy region. A non-perturbative treatment of the delta within ChPT was considered in Ref. [19], where the leading delta self-energy was resummed. However, a systematic resummation did not exist until the seminal work of Ref. [20], where it was justified by a power counting based on three separate scales  $m_\pi \ll \delta \ll M_{\text{QCD}}$ . This idea has since been applied to various electromagnetic reactions in the delta region [20–22], but for  $\pi N$  scattering few results have been published [22].

Note that other approaches exist to incorporate the delta (and other resonances) consistently with chiral symmetry and field-definition independence. They are reminiscent of the original approach [15, 23] to nucleon-nucleon interactions using chiral Lagrangians: a pion-nucleon “kernel” is first derived in ChPT to a certain order and then unitarized, for example using the  $N/D$  method [24] or the Bethe-Salpeter equation [25]. Power counting is not manifest at the amplitude level, but good results for pion-nucleon phase shifts are obtained past the delta region.

In this paper we realize the delta as a heavy baryon that fulfills Lorentz invariance order by order in powers of  $Q/m_N$ , using the nonrelativistic delta field as one of the building blocks. We employ a power counting developed for generic narrow resonances [26], previously applied to the shallowest  $P$ -wave resonance in nucleon-alpha particle scattering at very low energies [26, 27]. In this power counting we consider only two scales  $M_{\text{lo}} \sim \delta \sim m_\pi$  and  $M_{\text{hi}} \sim M_{\text{QCD}}$ , and expand in  $Q/M_{\text{hi}}$  and  $M_{\text{lo}}/M_{\text{hi}}$ . Certain contributions are enhanced near the resonance over the standard ChPT counting, which continues to apply near threshold. We can calculate the  $\pi N$  amplitude spanning the two regions in a controlled expansion. We illustrate the method by explicitly calculating the first three orders of the expansion and comparing with known  $P$ -wave phase shifts [28] and scattering volumes [29]. In the delta region our approach is similar, but not identical, to that in Ref. [20]. We compare our approach with those in Refs. [19, 20] as the differences arise.

The rest of the paper is organized as follows. In Sec. II we describe the heavy-baryon chiral Lagrangian that has an explicit delta field. (Some of the details of our implementation of the delta field are relegated to the Appendix.) We discuss the power counting in Sec. III. In Sec. IV we show how several key ingredients of the  $\pi N$  amplitude are calculated. The calculation and renormalization of the EFT amplitude are carried out in Sec. V. We then fit the  $P$ -wave phase shifts in Sec. VI. A summary of our results and a conclusion are offered in Sec. VII.

## II. EFFECTIVE LAGRANGIAN

In this section we briefly review how the effective Lagrangian is constructed. Much of this has already been discussed in the literature (see, *e.g.*, Refs. [3, 6, 7, 15]), our review here serving mainly to establish the notation. Some details about the delta can be found in the Appendix.

### A. Fields and symmetries

The effective Lagrangian, with hadronic degrees of freedom, is expected to exhibit the symmetries of QCD, which include Lorentz invariance, (approximate) parity and time-reversal invariance, color gauge symmetry, baryon-number conservation, and approximate  $SU(2)_L \times SU(2)_R$  chiral symmetry. Although it is possible to extend the theory to incorporate violations of parity and time-reversal, we neglect them here since they are small relative to the accuracy pursued by us. Generalization to  $SU(3)_L \times SU(3)_R$  is also possible.

Color gauge invariance is trivially satisfied in the EFT because hadrons are color singlets. Baryon number conservation requires baryons to appear in bilinears. In the kinematic region where the EFT holds, external momenta are much smaller than the nucleon mass,  $Q \ll m_N$ , and thus Lorentz invariance can be fulfilled perturbatively in powers of  $Q/m_N$ . There are two approaches in the literature to build the corresponding effective Lagrangian. One approach is to write a relativistic Lagrangian and then to derive the  $Q/m_N$  expansion by integrating out high-energy components using the path integral [30]. In the case of the delta [14, 20], one uses a Rarita-Schwinger field. The so-called “off-shell” parameters that control the spurious spin-1/2 sectors of the Rarita-Schwinger field are interpreted as choices of “gauge”. By building a gauge-invariant Lagrangian and choosing a certain gauge in Feynman rules, the spurious spin-1/2 sectors can be removed from the final result.

It is not, however, inevitable to rely on the form of a Lagrangian outside the regime of validity of an EFT; only the symmetries should be important. Since in the region where ChPT is valid the nucleon and delta are always nonrelativistic, the other approach [13, 15] starts from the nonrelativistic limit. This is accomplished by using heavy-fermion fields  $N$  for the nucleon and  $\Delta$  for the delta, which are, respectively, two- and four-component spinors in spin ( $S$ ) and isospin ( $I$ ) spaces. Compared to the relativistic fields, the heavy-fermion fields have the common, inert, large mass  $m_N$  removed, and contain only the destruction of particles. Not only does the heavy-baryon formalism keep clear track of the small expansion parameter,  $Q/m_N$ , but it also is convenient as a framework to write the most general effective Lagrangian, where the only baryon degrees of freedom are those representing forward propagation.

As usual, we introduce the spin operators  $\vec{S}^{(S)}$ , normalized so that

$$[S_i^{(S)}, S_j^{(S)}] = i\epsilon_{ijk} S_k^{(S)}, \quad (2)$$

and in isospace  $\mathbf{t}^{(I)}$ , normalized the same way. We write  $\vec{S}^{(\frac{1}{2})} = \vec{\sigma}/2$  and  $\mathbf{t}^{(\frac{1}{2})} = \vec{\tau}/2$  in terms

of Pauli matrices. One also needs transition matrices that have proper Clebsch-Gordan (CG) coefficients embedded. We define  $2 \times 4$  matrices  $S_i$  in spin space such that their matrix elements between a nucleon state with a spin  $z$ -component  $\sigma$  and a delta state with a spin  $z$ -component  $s$  are

$$(S_i)_{\sigma s} \equiv \langle 1\frac{1}{2}; \sigma | 1\frac{1}{2}; \frac{3}{2} s \rangle, \quad (3)$$

where we use the notation of Ref. [31]. It is not difficult to show that the bilinear  $N^\dagger \vec{S} \Delta$  is a three-vector, thanks to the Wigner-Eckart theorem. We impose the normalization condition

$$S_i S_j^\dagger = \frac{1}{3} (2\delta_{ij} - i\epsilon_{ijk} \sigma_k). \quad (4)$$

In addition, there is a spin-2 bilinear,  $N^\dagger \Omega_{ij} \Delta$ , which is a symmetric, traceless three-tensor, with

$$(\Omega_{ij})_{\sigma s} \equiv \langle 2\frac{1}{2}; \sigma | i j | 2\frac{1}{2}; \frac{3}{2} s \rangle = \frac{1}{2} (\sigma_i S_j + \sigma_j S_i)_{\sigma s}. \quad (5)$$

Similar transition matrices,  $\mathbf{T}$  and  $\Xi_{ab}$ , can be defined in isospace such that  $N^\dagger \mathbf{T} \Delta$  and  $N^\dagger \Xi_{ab} \Delta$  are an isovector and an isotensor, respectively.

In order to build the effective Lagrangian, one first enumerates all the rotation-invariant operators and then uses a Lorentz transformation rule perturbative in slow-velocity boosts to constrain the coefficients of those operators. However, it is not yet clear how one can go beyond order  $Q/m_N$  with this “bottom-up” approach. A separate paper by one of us [32] addresses this issue: the systematic construction of a deltaful, heavy-baryon chiral Lagrangian with arbitrarily high relativistic corrections. The Appendix summarizes the aspects of Ref. [32] relevant for the current paper. In essence, we implement baryons via the Foldy-Wouthuysen representation [33] of the Poincaré group, whose boost generators can be readily expanded in powers of  $Q/m_N$ .

Chiral symmetry is more complicated to implement because it is spontaneously broken by the QCD vacuum to its isospin subgroup, and it is thus nonlinearly realized in terms of pion and baryon fields [3, 34, 35]. Here we use stereographic coordinates  $\boldsymbol{\pi}$  to represent the isovector pion field [3, 15, 34], for which we define a covariant derivative

$$\mathbf{D}_\mu \equiv D^{-1} \frac{\partial_\mu \boldsymbol{\pi}}{2f_\pi}, \quad (6)$$

with  $f_\pi \simeq 92$  MeV the pion decay constant and

$$D \equiv 1 + \frac{\boldsymbol{\pi}^2}{4f_\pi^2}. \quad (7)$$

The nonlinear realization maps axial chiral-rotations of  $N$ ,  $\Delta$ , and  $\mathbf{D}_\mu$  into  $\boldsymbol{\pi}$ -dependent (hence “local”) isospin rotations [3, 34, 35]. Since such local isospin rotations do not commute with normal

derivatives, one also needs covariant derivatives for  $N$ ,  $\Delta$ , and  $\mathbf{D}_\mu$ . For a generic chiral-covariant field with isospin  $I$ ,  $\psi^{(I)}$ , its covariant derivative is defined as [3, 15, 34]

$$\mathcal{D}_\mu \psi^{(I)} \equiv \left( \partial_\mu + \mathbf{t}^{(I)} \cdot \mathbf{E}_\mu \right) \psi^{(I)}, \quad (8)$$

where

$$\mathbf{E}_\mu \equiv i \frac{\pi}{f_\pi} \times \mathbf{D}_\mu. \quad (9)$$

For an isovector with Cartesian indices like  $\mathbf{D}_\nu$ , it is conventional to write the covariant derivative as

$$\mathcal{D}_\mu \mathbf{D}_\nu \equiv \partial_\mu \mathbf{D}_\nu + i \mathbf{E}_\mu \times \mathbf{D}_\nu. \quad (10)$$

Any isospin-invariant operator made of  $N$ ,  $\Delta$ ,  $\mathbf{D}_\mu$  and their covariant derivatives will automatically be  $SU(2)_L \times SU(2)_R$  invariant.

Explicit chiral-symmetry breaking induced by the quark masses can easily be incorporated in the effective Lagrangian. Those operators, denoted by  $\Phi^\pm$ , that are proportional to  $m_u \pm m_d$  will have a structure as follows [3, 15, 34],

$$\Phi^+ = -D^{-1} \frac{\pi}{f_\pi} \cdot \boldsymbol{\eta}^+ + D^{-1} \left( 1 - \frac{\pi^2}{4f_\pi^2} \right) \eta_4^+, \quad (11)$$

$$\Phi^- = \left( \eta_3^- - \frac{1}{2} D^{-1} \frac{\pi_3}{f_\pi} \frac{\pi}{f_\pi} \cdot \boldsymbol{\eta}^- \right) + D^{-1} \frac{\pi_3}{f_\pi} \eta_4^-, \quad (12)$$

where the quantities  $\boldsymbol{\eta}^\pm$  and  $\eta_4^\pm$  are built of covariant fields and are isovector and isoscalar, respectively. To preserve parity, it is easy to show that  $\boldsymbol{\eta}^+$  ( $\boldsymbol{\eta}^-$ ) and  $\eta_4^-$  ( $\eta_4^+$ ) are pseudoscalar (scalar). It can be shown [15] that isospin is an accidental symmetry, in the sense that it only appears in the subleading effective Lagrangian. As a first study, we focus here on the isospin-invariant part of the  $\pi N$  amplitude.

Electromagnetic interactions can be easily incorporated in the Lagrangian by adding the requirement of  $U(1)$  gauge invariance. This is accomplished by turning all derivatives in existing interactions into gauge-covariant derivatives, and by adding additional gauge-invariant interactions with the electromagnetic field strength. Here for simplicity we neglect electromagnetic interactions.

## B. Effective Lagrangian

Since the effective Lagrangian has an infinite number of interactions, one needs a scheme to organize all its operators. It is convenient to order the Lagrangian terms according to the so-called

chiral index  $\nu$  [5],

$$\nu = d + m + n_\delta + \frac{f}{2} - 2 \geq 0, \quad (13)$$

where  $d$ ,  $m$ ,  $n_\delta$  and  $f$  are the numbers of derivatives, powers of  $m_\pi$ , powers of  $\delta$  and fermion fields, respectively. The lowest value of the index is a consequence of the pattern of chiral-symmetry breaking in QCD.

In constructing the Lagrangian, we use integration by parts and field redefinitions to remove time derivatives on baryon fields except for the kinetic terms. The Lagrangian terms with the two lowest indices are given by [15]

$$\begin{aligned} \mathcal{L}^{(0)} = & 2f_\pi^2 \mathbf{D}^2 - \frac{m_\pi^2}{2D} \boldsymbol{\pi}^2 + N^\dagger i \mathcal{D}_0 N + g_A N^\dagger \boldsymbol{\tau} \vec{\sigma} N \cdot \vec{\mathbf{D}} \\ & + \Delta^\dagger (i \mathcal{D}_0 - \delta) \Delta + 4g_A^\Delta \Delta^\dagger \mathbf{t}^{(\frac{3}{2})} \vec{S}^{(\frac{3}{2})} \Delta \cdot \vec{\mathbf{D}} + h_A \left( N^\dagger \mathbf{T} \vec{S} \Delta + H.c. \right) \cdot \vec{\mathbf{D}} + \dots \end{aligned} \quad (14)$$

and

$$\begin{aligned} \mathcal{L}^{(1)} = & N^\dagger \frac{\vec{\mathcal{D}}^2}{2m_N} N + 2c \frac{m_\pi^2}{D} \boldsymbol{\pi}^2 N^\dagger N + \Delta^\dagger \left[ \frac{\vec{\mathcal{D}}^2}{2m_N} - (c^\Delta - c) m_\pi^2 \right] \Delta + 2c^\Delta \frac{m_\pi^2}{D} \boldsymbol{\pi}^2 \Delta^\dagger \Delta \\ & - \frac{h_A}{m_N} \left( i N^\dagger \mathbf{T} \vec{S} \cdot \vec{\mathcal{D}} \Delta + H.c. \right) \cdot \mathbf{D}_0 + \dots, \end{aligned} \quad (15)$$

while the next-higher index yields

$$\begin{aligned} \mathcal{L}^{(2)} = & -\frac{\Delta m_\pi^2}{2D^2} \boldsymbol{\pi}^2 - \frac{\delta}{2m_N^2} \Delta^\dagger \vec{\mathcal{D}}^2 \Delta + \frac{h_A}{2m_N^2} \left[ \left( N^\dagger \mathbf{T} \vec{S} \vec{\mathcal{D}}^2 \Delta - N^\dagger \mathbf{T} \vec{S} \cdot \vec{\mathcal{D}} \vec{\mathcal{D}} \Delta \right) + H.c. \right] \cdot \vec{\mathbf{D}} \\ & + \frac{h_A}{8m_N^2} \left[ \left( \delta_{lm} N^\dagger \mathbf{T} \vec{S} \cdot \vec{\mathcal{D}} \Delta + 3N^\dagger \mathbf{T} S_l \mathcal{D}_m \Delta - 2i\epsilon_{ijl} N^\dagger \mathbf{T} \Omega_{im} \mathcal{D}_j \Delta \right) + H.c. \right] \cdot \mathcal{D}_l \mathbf{D}_m \\ & + d \frac{m_\pi^2}{D} \left( 1 - \frac{\boldsymbol{\pi}^2}{4f_\pi^2} \right) \left( N^\dagger \mathbf{T} \vec{S} \Delta + H.c. \right) \cdot \vec{\mathbf{D}} + \dots \end{aligned} \quad (16)$$

Here,  $g_A$  ( $g_A^\Delta$ ) is the  $\nu = 0$  axial-vector coupling of the nucleon (delta) and  $h_A$  ( $d$ ) is the  $\nu = 0$  ( $\nu = 2$ )  $\pi N \Delta$  coupling. These low-energy constants (LECs) are expected to be of  $\mathcal{O}(1/M_{\text{QCD}}^\nu)$  but are not determined by chiral symmetry. We define the phases of pion and delta fields so that  $g_A \geq 0$  and  $h_A \geq 0$ . The  $\Delta m_\pi^2$  term provides a correction to the pion mass that is proportional to the square of the average quark mass (it is related to the  $l_3$  term in Ref. [5]); in the following, in order to simplify formulas, we absorb its contribution in  $m_\pi^2$ . Likewise, the nucleon and delta masses receive at  $\nu = 1$  contributions that are linear in the average quark mass, the respective sigma terms (see, *e.g.*, Ref. [36]) denoted here by  $c$  and  $c^\Delta$ . With our choice of heavy-nucleon field we have already absorbed  $cm_\pi^2$  in the nucleon mass  $m_N$ . Again, for simplicity, in the following we absorb the remaining mass contribution,  $(c^\Delta - c)m_\pi^2$ , in  $\delta$ . The remaining pion-delta interaction,



together with a number of other interactions not shown, contributes to the order we work below only to a further renormalization of  $\delta$ . The interactions associated with the pion and nucleon mass corrections only contribute to our reaction at higher order. Note that “ $\dots$ ” refer to terms that do not appear explicitly in  $\pi N$  scattering to the order concerned in this paper. Higher-index Lagrangians can be constructed with more derivatives, but will also only contribute at higher orders.

Different versions of the heavy-baryon effective Lagrangian that are deduced from a relativistic formalism are given in Refs. [14, 18]. Their Lagrangians, in our notation, both have an independent  $\nu = 1$   $\pi N\Delta$  coupling (denoted by  $b_3$  and  $b_3 + b_8$  respectively in Refs. [14] and [18]). This is because redundancy due to baryonic equations of motion is only removed at the relativistic level in Refs. [14, 18], and further minimization of the number of interactions due to the heavy-baryon equations of motion is not considered there. The  $d$  term in Eq. (16) is equivalent to the combination of couplings  $-2f_4 + f_5$  in Ref. [18].

### III. POWER COUNTING

We now turn to the ordering of contributions to physical processes. For definiteness we take  $\pi N$  elastic scattering, although the power counting is the same for other one-nucleon reactions where the external CM energy can be dialed to near the delta-nucleon mass splitting. We consider throughout the case  $Q \sim m_\pi \sim \delta \ll M_{\text{QCD}}$ .

#### A. Away from the resonance

We first consider CM energies much below the delta peak. In this case power counting is standard [5–7] with the simple generalization that  $\delta$  counts as  $Q$ . The contribution of a diagram with  $A$  nucleons (here  $A = 1$ ),  $L$  loops, and  $V_i$  vertices with chiral index  $\nu_i$  is proportional to  $Q^\rho$ , with

$$\rho = 2 - A + 2L + \sum_i V_i \nu_i \geq 2 - A. \quad (17)$$

The contributions with minimum  $\rho$  form the leading order (LO), the next contributions are referred to as next-to-leading order (NLO), and so on.

The power counting can also be applied to sub-diagrams if  $A$  is generalized to count any fermion line that is unattached on one side. Examples, which will be important later, are the following:



FIG. 1: The LO pion self-energy,  $\Sigma_\pi^{(0)}$ . A dashed line represents a free pion propagator. The unmarked vertex has  $\nu = 0$  and the twice-circled vertex has  $\nu = 2$ .

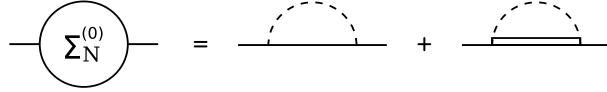


FIG. 2: The LO nucleon self-energy,  $\Sigma_N^{(0)}$ . A single (double) line represents a free nucleon (delta) propagator. Vanishing diagrams are not shown.

(i) The LO contribution to the pion self-energy  $\Sigma_\pi^{(0)} = \mathcal{O}(Q^4/M_{\text{QCD}}^2)$ , see FIG. 1, two powers down compared to the inverse of the free pion propagator. From the LO pion self-energy we obtain a correction to the pion-field renormalization constant,  $Z_\pi^{(2)} = \mathcal{O}(Q^2/M_{\text{QCD}}^2)$ .

(ii) The LO contribution to the nucleon self-energy  $\Sigma_N^{(0)} = \mathcal{O}(Q^3/M_{\text{QCD}}^2)$ , see FIG. 2, two powers down from the nucleon kinetic energy. From the LO nucleon self-energy we obtain a correction to the nucleon-field renormalization constant,  $Z_N^{(2)} = \mathcal{O}(Q^2/M_{\text{QCD}}^2)$ .

(iii) The LO contribution to the delta self-energy  $\Sigma_\Delta^{(0)} = \mathcal{O}(Q^3/M_{\text{QCD}}^2)$ , see FIG. 3, two powers down from the delta kinetic energy and delta-nucleon mass difference. From the LO delta self-energy we can define a correction to the delta-field renormalization constant,  $Z_\Delta^{(2)} = \mathcal{O}(Q^2/M_{\text{QCD}}^2)$ .

(iv) The NLO contribution to the delta self-energy  $\Sigma_\Delta^{(1)} = \mathcal{O}(Q^4/M_{\text{QCD}}^3)$ , see FIG. 4.

(v) The NNLO contribution to the delta self-energy  $\Sigma_\Delta^{(2)} = \mathcal{O}(Q^5/M_{\text{QCD}}^4)$ , see FIG. 5.

(vi) The NNLO contribution to the  $\pi N \Delta$  vertex form-factor  $V_\pi^{(2)} = \mathcal{O}(Q^3/M_{\text{QCD}}^2)$ , see FIG. 6, two powers down from the  $\nu = 0$   $h_A$  vertex.

This power counting holds for generic momenta, but it does not work equally well in every specific region of phase space. For example, close to threshold an incoming or outgoing pion has energy very close to  $m_\pi$  and a three-momentum close to zero—it is, in other terms, nonrelativistic. In such cases, a spatial derivative on the pion field does not contribute the same as a time derivative, yet Eq. (17) does not discriminate between these derivatives. One can refine power counting for

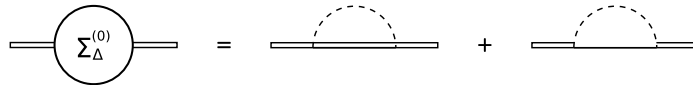


FIG. 3: The LO delta self-energy,  $\Sigma_\Delta^{(0)}$ . Vanishing diagrams are not shown.

FIG. 4: The NLO correction to the delta self-energy,  $\Sigma_{\Delta}^{(1)}$ . The once-circled vertices have  $\nu = 1$ . Vanishing diagrams are not shown.

FIG. 5: The NNLO correction to the delta self-energy,  $\Sigma_{\Delta}^{(2)}$ . The twice-circled vertices have  $\nu = 2$ . Vanishing diagrams are not shown.

this region if one wishes.

## B. Near the resonance

It should thus be no surprise that the above power counting fails in the immediate neighborhood of the delta resonance. Consider the two contributions to  $\pi N$  scattering in FIG. 7 at a CM energy  $E$ . Diagram (a) is proportional to  $1/(E - \delta)$  and diagram (b) to  $\Sigma_{\Delta}^{(0)}(E)/(E - \delta)^2$ , which

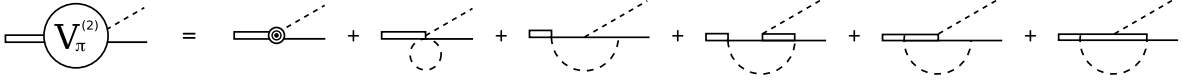


FIG. 6: The NNLO correction to the  $\pi N\Delta$  vertex,  $V_\pi^{(2)}$ . Vanishing diagrams are not shown.

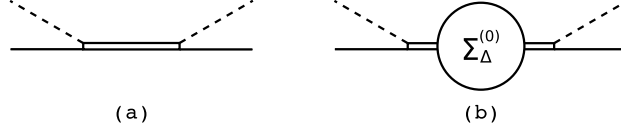


FIG. 7: Examples of one- $\Delta$ -reducible diagrams.

are, respectively,  $\mathcal{O}(1/Q)$  and  $\mathcal{O}(Q/M_{\text{QCD}}^2)$  at a generic low energy. Although both  $E$  and  $\delta$  are separately of  $\mathcal{O}(Q)$ , they have opposite signs and can cancel. When that happens, diagrams (a) and (b) are enhanced above their standard power counting, and diagram (b) is enhanced more than (a) so that the self-energy might no longer be a small correction: a resummation is necessary. The situation here is completely analogous to other narrow resonances [26], where a “kinematic fine-tuning” requires a modification of power counting in the neighborhood of a resonance.

In fact, within a window of size

$$|E - \delta| = \mathcal{O}\left(\frac{Q^3}{M_{\text{QCD}}^2}\right) \quad (18)$$

around the delta peak, the bare delta propagator is  $\mathcal{O}(M_{\text{QCD}}^2/Q^3)$ . Since  $\Sigma_\Delta^{(0)}$  is  $\mathcal{O}(Q^3/M_{\text{QCD}}^2)$ , one simultaneous insertion of  $\Sigma_\Delta^{(0)}$  and the bare delta propagator contributes  $\mathcal{O}(1)$ , so the two diagrams in FIG. 7 become comparable. We should thus resum the geometric series of one- $\Delta$ -reducible delta propagators shown in FIG. 8. Moreover, since within the window  $E = \delta(1 + \mathcal{O}(Q^2/M_{\text{QCD}}^2))$ , the energy dependence of  $\Sigma_\Delta(E)$  is always two powers down from its value at  $E = \delta$ :

$$\Sigma_\Delta^{(n)}(E) = \Sigma_\Delta^{(n)}(\delta) \left\{ 1 + \mathcal{O}\left(\frac{Q^2}{M_{\text{QCD}}^2}\right) \right\}. \quad (19)$$

The resummation thus amounts to a dressed propagator

$$S_\Delta^{(0)}(E) = \left[ E - \delta + \Sigma_\Delta^{(0)}(\delta) \right]^{-1}, \quad (20)$$

which scales as  $M_{\text{QCD}}^2/Q^3$ . This is an enhancement of two powers over the generic situation. To make a full amplitude, one needs to contract the dressed propagators with the  $\pi N\Delta$  vertices, for which we should also neglect the energy dependence:

$$V_\pi^{(n)}(E) = V_\pi^{(n)}(\delta) \left\{ 1 + \mathcal{O}\left(\frac{Q^2}{M_{\text{QCD}}^2}\right) \right\}. \quad (21)$$

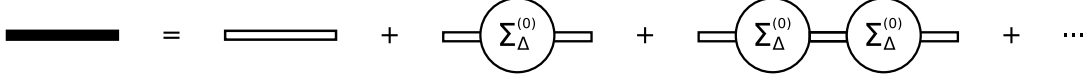


FIG. 8: Dressed delta propagator at LO as a sum of insertions of  $\Sigma_{\Delta}^{(0)}$ .

In contrast, in one- $\Delta$ -irreducible diagrams the delta propagators are far away from their pole and do not need to be dressed, continuing to scale as  $1/Q$ . This is trivial in one- $\Delta$ -irreducible trees, *e.g.*, the  $u$ -channel  $\Delta$ -exchange diagram. Less trivial are the loop diagrams where there are integrations over the energy domain spanning the delta pole. In this case, pions in the loops carry at least  $m_{\pi}$  of energy, and the delta will not go on-shell for  $\pi N$  energies below  $\delta + m_{\pi}$ . Even at this point, the delta will be recoiling and the kinetic energy needs to be taken into account before the self-energy.

Take for example the one-loop diagrams with a delta that contribute to the LO nucleon (FIG. 2) and delta (FIG. 3) self-energies. Suppose that the external fermion and the internal pion have four-momentum  $p$  and  $l$ , respectively. Apart from the CG coefficients and coupling constants in front, the loop integral with the bare dressed propagator has the form

$$\int \frac{d^3l}{(2\pi)^3} \int \frac{dl_0}{2\pi} \frac{\vec{l}^2}{p_0 - l_0 - \delta + i\epsilon} \frac{1}{l^2 - m_{\pi}^2 + i\epsilon}. \quad (22)$$

One can always close the contour of integration over  $l_0$  in the half-plane opposite to the half-plane where the pole of the delta propagator is. In this case, we pick the pole at  $l_0 = \omega - i\epsilon$ , where  $\omega = \sqrt{\vec{l}^2 + m_{\pi}^2}$  is the pion energy. The remaining integral over  $\vec{l}$  has no singularities when  $p_0 = \delta$ . Alternatively, rewriting it as an integral over  $\omega$  after carrying out the angular integrations, it starts at  $m_{\pi}$  while the integrand has poles only at  $\omega = 0$  and  $\omega = p_0 - \delta$ . The same argument holds for  $A = 1$  diagrams with more loops.

As a consequence, in one-delta-irreducible diagrams the standard ChPT power counting (17) still applies; dressed delta propagators only need to be included in one-delta-reducible diagrams. We thus arrive at a new power counting for one- $\Delta$ -reducible diagrams within a narrow window around the delta peak,

$$\rho = 2 - A - 2n_{\Delta} + 2L + \sum_i V_i \nu_i \geq 2 - A - 2n_{\Delta}, \quad (23)$$

where  $n_{\Delta}$  is the number of dressed delta propagators. This is the non-electromagnetic version of  $\rho$  derived in a slightly different power counting in Ref. [20]. We discuss the similarities and differences between the two approaches in Sec. III D.

Notice that there is a larger region around the resonance, of size  $|E - \delta| = \mathcal{O}(Q^2/M_{\text{QCD}})$ , where the enhancement in the delta propagator is insufficient to compensate for an insertion of the self-energy. Although the power counting is slightly different than Eq. (17), this case is still perturbative. For simplicity, we do not consider it separately from the generic situation away from the resonance, where  $|E - \delta| = \mathcal{O}(Q)$ .

### C. Sewing the two regions

We can now weigh the diagrams contributing to  $\pi N$  scattering, putting together the two power countings (17) in the off-the-pole region and (23) in the pole region. These contributions generally scale as  $\mathcal{O}(Q^\rho/M_{\text{QCD}}^{\rho-1}f_\pi^2)$ , where  $1/f_\pi^2$  is due to the two pion external legs. Without causing confusion, we simply specify the size of the contribution of a  $\pi N$  scattering diagram by order “ $Q^\rho$ ”. Found in FIG. 9 are diagrams up to order  $Q^1$ . To this order, the kinematic fine-tuning to the delta simply promotes the diagrams on the right (labeled A, B, C) of the figure with respect to the standard assignment on the left (D). The diagrams at the bottom (E), which are one-delta irreducible, are not affected.

It seems that the two different power-counting schemes, which are applicable in two different regions, would lead to an EFT amplitude in the form of a piecewise function in the energy. Even worse, separating these two regions is somewhat arbitrary.

A piecewise EFT is actually unnecessary. Look at, for instance, the  $Q^{-1}$  order. Only the LO pole diagram (FIG. 9(A)) contributes at this order. Since there is no diagram in the off-the-pole region, the EFT prediction should vanish when away from the pole. Enforcing the LO pole diagram in the off-the-pole region seems to make a “wrong” prediction. However, it is only wrong by an amount of order  $Q^1$ , since a dressed delta propagator scales off-pole as a bare one ( $E - \delta$  dominates over  $\Sigma_\Delta^{(0)}$ ). This is of the same order as the tree in FIG. 9(D). On the other hand, however, one already made an even larger error of order  $Q^0$  by neglecting the NLO pole diagrams. To put it another way, extending the domain of the LO pole diagram is equivalent to shifting a subset of higher diagrams into the order  $Q^{-1}$ . This does not disobey the original power counting as long as one does not claim a higher accuracy by doing so. In many perturbative quantum field theories, one runs the renormalization group to select an optimal renormalization scale in favor of a more rapid convergence of the perturbative series, which is also equivalent to a rearrangement of diagrams.

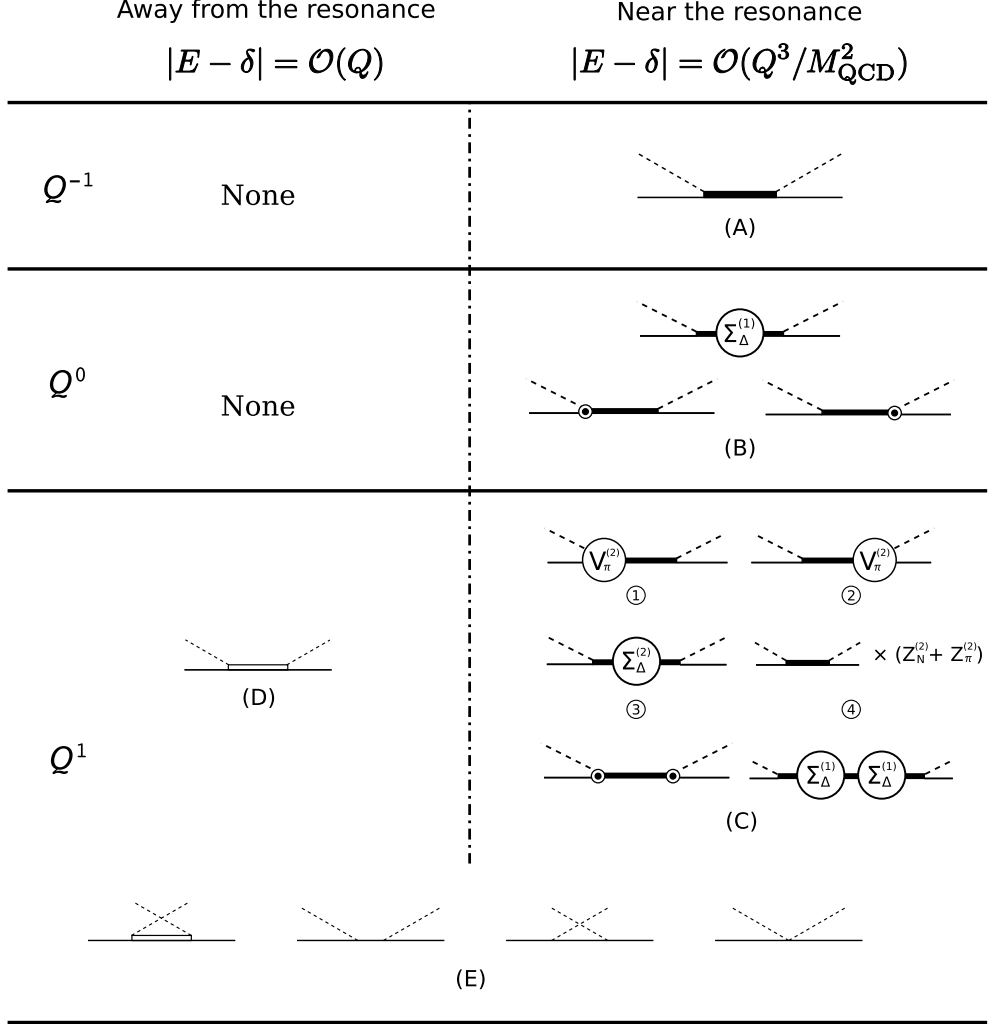


FIG. 9: Contributions to  $\pi N$  scattering up to order  $Q^1$ : (A)  $Q^{-1}$  pole diagram; (B)  $Q^0$  pole diagrams; (C)  $Q^1$  pole diagrams; (D)&(E)  $Q^1$  tree diagrams, of which (E) apply to both regions. Power counting away from the resonance is the standard ChPT counting. The relation between the double line (bare delta propagator) and the thick solid line (dressed delta propagator) is given in Fig. 8.

This sort of rearrangement, written symbolically as

$$N^\alpha \text{LO} + \text{a subset of } \sum_{i>\alpha} N^i \text{LO} \rightarrow N^\alpha \text{LO}, \quad (24)$$

must be used with caution. First, the higher-order subset being added to  $N^\alpha \text{LO}$  should be cutoff-independent by itself, in order to avoid introducing model dependence in the form of cutoff dependence. Second, one probably would not like to move undetermined LECs into lower orders because doing so weakens the predictive power of EFT. In our case, order-by-order renormalizability of the rearranged diagrams will be relatively simple to demonstrate because, in the resonance counting, energy variation in the delta self-energy and interaction vertices is treated perturbatively. We will

also see that the rearranged diagrams include in the off-pole region, within an error of order  $Q^2$ , only delta parameters that appear in the diagrams of FIG. 9(D,E).

Ensuring that our amplitude is correct also away from the resonance region does require some care. When the pion and nucleon in the initial and final states are on-shell, the momentum dependences in the  $\pi N\Delta$  external vertices translate into energy dependence. In the resonance counting, such energy dependence is subject to  $E = \delta + \mathcal{O}(Q^3/M_{\text{QCD}}^2)$  so that the  $\pi N\Delta$  external vertices in the LO and NLO pole diagrams are constant. This has two consequences. (i) Up to order  $Q^0$  the  $P$ -wave amplitude in the delta channel does not vanish at threshold as it should. But, as we argued, applying the LO pole diagram near threshold is expected to make an error of order  $Q^1$ , which can be taken as “vanishing” in comparison with the dominant amplitude around the resonance. (ii) Since the energy expansion around  $\delta$  should not be enforced in FIG. 9(D), simply continuing the LO pole diagram away from the resonance would not reproduce FIG. 9(D) due to the lack of energy dependence in the external vertices. To account for FIG. 9(D), the easiest way is to restore at order  $Q^1$  the energy dependence of the external vertices of FIG. 9(A).

To summarize, with sufficient caution it is unnecessary to restrict the energy domain of the dressed pole diagrams in FIG. 9. Of course, our power counting stresses the fact that amplitudes are much larger in the resonance region than at threshold. If one is interested solely in the region near threshold, where the delta enhancement is not relevant, one is better off with the standard ChPT power counting—or, for reactions where typical three-momenta are below the pion mass, with a “heavy-pion” EFT [37]. Using our power counting in both threshold and resonance regions is only efficient if one aims for a unified description throughout the low-energy region.

#### D. Other approaches

The above power counting is not limited to  $\pi N$  scattering. It applies to any reaction where one can dial the initial energy to bring the delta close to being on-shell. Of course, the need to account for the delta self-energy has been felt for a very long time, and simple tree-level models with an added delta self-energy already provide at least qualitative descriptions of data [38]. What EFT provides in addition is a way, consistent with QCD symmetries, to correct systematically for quantum effects and physics at short distances. We now compare our power counting to other approaches that considered non-perturbative effects of the delta in EFT.

Reference [19] resummed the LO delta self-energy in one-delta-reducible diagrams (as done here), and used the corresponding delta width as an independent empirical input. The scheme



is quite different from ours. First, it did not take into account the fact that the dressed delta propagator is enhanced by  $\mathcal{O}(M_{\text{QCD}}^2/Q^2)$  in the resonance region, and hence adopted the standard ChPT power counting except for simply substituting the LO dressed delta propagator for the bare one. Therefore, the off-the-pole region was excessively emphasized with a two-order-higher accuracy than the resonance region. This discrepancy in power counting may be viewed as a rearrangement of the type (24) but Ref. [19] enlisted many more LECs to achieve the same overall accuracy. Second, perhaps more importantly, Ref. [19] did not consider the corrections to the delta self-energy. For instance, in our power counting the one-loop corrections to the  $\pi N\Delta$  vertex,  $V_\pi^{(2)}$  defined in FIG. 6, contribute to the NNLO pole diagrams not only through vertices attached to external legs but also in  $\Sigma_\Delta^{(2)}$ . The latter, however, were neglected in Ref. [19]. This would make one, if using the scheme in Ref. [19], unable to recover Eq. (1) around the resonance, which is required by order-by-order unitarity. The difficulty of preserving unitarity around the resonance forced Ref. [19] to rely on certain prescriptions, referred to as  $S$ - or  $K$ -matrix method therein, to extract the phase shifts from the scattering amplitude. In particular, one of the prescriptions, the  $S$ -matrix method, leads to a discontinuity in the phase shifts.

More sophisticated methods of unitarization based on EFT exist, for example Refs. [24, 25]. In this case, if a sufficiently high-order kernel is fully iterated in an analogous fashion to what is done in the two-nucleon system [7, 15, 23], corrections to the leading delta self-energy are accounted for and good results can be obtained even beyond the delta resonance. However, in a system with two heavy particles of reduced mass  $\mu$  such a unitarization is justified by an infrared enhancement of  $\mathcal{O}(4\pi\mu/Q)$  over the standard ChPT counting [7]. While this might apply to the strangeness sector of ChPT, the strict EFT rationale for resummation in pion-nucleon scattering in the resonance region must be rooted in arguments such as those in Refs. [20–22] and in the present manuscript. Contrary to Ref. [19], the resummations in Refs. [20–22] are based on a power counting very similar to ours. Both in Refs. [20–22] and here, it is recognized that the immediate vicinity of the resonance requires a different power counting than the one in standard ChPT. Moreover, in both approaches there is an attempt to smoothly bridge the resonance region with lower energies.

Our power counting differs from the one proposed in Ref. [20], however, in that  $\delta$  was assumed in Ref. [20] to be much larger than  $m_\pi$ ,  $m_\pi/M_{\text{QCD}} \sim (\delta/M_{\text{QCD}})^2$ . As a consequence, the relative importance of explicit chiral-symmetry-breaking terms is reduced. Strictly speaking, in the light of the hierarchy  $m_\pi \ll \delta$ , one would have to neglect the  $m_\pi^2$  in the pion propagator in  $\Sigma_\Delta^{(0)}$  and other diagrams where the pion momentum is  $\mathcal{O}(\delta)$ . This might lead to unpleasant infrared divergences in certain diagrams, which Ref. [20] avoids by not enforcing their power counting in the calculation

of diagrams. Of course this can be justified by a rearrangement in the fashion of Eq. (24), and if this is done it blurs the difference between the two power countings somewhat.

Clearly, as emphasized by the authors, the power counting of Ref. [20] is well-suited to study the regime of smaller quark masses, where  $m_\pi$  decreases but  $\delta$  is basically unchanged. In contrast, it works less well as the number of colors  $N_c$  increases, when  $\delta$  decreases. In any case, in the real world the scales are not clearly separated,  $\delta$  being larger than  $m_\pi$  only by a factor of  $\sim 2$ , and the interesting limits  $m_\pi \rightarrow 0$  and  $N_c \rightarrow \infty$  can always be studied separately afterwards.

Thus, if one is going to generically treat the pion mass as comparable to momenta in loops around the resonance, we find it simpler not to emphasize such a factor of 2, given that there are lots of other similar factors floating around. We simply count  $\delta$  as comparable to the  $m_\pi$ ,  $m_\pi/M_{\text{QCD}} \sim \delta/M_{\text{QCD}}$ , as it has been done before away from the resonance [13–18].

This discussion about the best way to power-count explicit-symmetry-breaking terms should not obscure—as it apparently has—the important fact that it is the kinematic fine-tuning to a narrow resonance (that is, one that has a width smaller than its energy) that demands a resummation [20]. This is in fact quite a general requirement of an EFT for shallow resonances [26], which has nothing to do with explicit chiral-symmetry breaking.

#### IV. ONE-DELTA-IRREDUCIBLE INGREDIENTS

As an example of our approach, we want to calculate the  $\pi N$   $T$  matrix to  $\mathcal{O}(Q^1)$ . The tree diagrams are straightforward, but the pole diagrams in FIG. 9 are more complicated. The latter have three common components: the field renormalization constants  $Z_\pi$  and  $Z_N$ , the  $\pi N \Delta$  vertex function  $V_\pi$ , and the delta self-energy  $\Sigma_\Delta$ . All of these ingredients are made up of one- $\Delta$ -irreducible graphs, which can be expanded in powers of  $Q/M_{\text{QCD}}$  according to the standard ChPT power counting. In this section we investigate each of the ingredients in turn, up to relative  $\mathcal{O}(Q^2/M_{\text{QCD}}^2)$ .

Note that in general these quantities are cutoff-dependent. If dimensional regularization (DR) is used, cutoff dependences in the loops appear as  $1/(D-4)$  poles in the complex dimensionality ( $D$ ) plane near  $D=4$ . Of course, the scattering amplitude should be independent of any cutoff. Therefore, the cutoff dependences must be absorbed by suitable counterterms.

### A. Field renormalization constants

Field renormalization constants  $Z_\pi$  and  $Z_N$  are the residues of the corresponding two-point Green's function (or fully dressed propagator).

The renormalized pion mass is the magnitude of the momentum of the pole of the dressed pion propagator, which we denote by  $m_\pi$ . At the pole, the pion four-momentum  $p$  obeys  $p_0 = \omega(|\vec{p}|)$ , the energy of an on-shell pion:

$$\omega(|\vec{p}|) \equiv \sqrt{\vec{p}^2 + m_\pi^2}. \quad (25)$$

The pion self-energy,  $\Sigma_\pi(p^2)$ , is such that  $\Sigma_\pi(m_\pi^2) = 0$ . The pion field renormalization constant  $Z_\pi$  is related to  $\Sigma_\pi(p^2)$  by

$$Z_\pi^{-1} = 1 + \left. \frac{d}{dp^2} \Sigma_\pi(p^2) \right|_{p^2=m_\pi^2}. \quad (26)$$

Expanding in powers of  $Q/M_{\text{QCD}}$  according to the standard ChPT power counting, to NNLO,

$$Z_\pi^{(0)} = 1, \quad (27)$$

$$Z_\pi^{(1)} = 0, \quad (28)$$

$$Z_\pi^{(2)} = - \left. \frac{d}{dp^2} \Sigma_\pi^{(0)}(p^2) \right|_{p^2=m_\pi^2}, \quad (29)$$

where  $\Sigma_\pi^{(0)}$  is the LO pion self-energy shown in FIG. 1.

Similarly, we renormalize the nucleon mass in such a way that the pole of the dressed propagator of a nucleon of four-momentum  $p$  is given by  $p_0 = E_N(|\vec{p}|)$ , where

$$E_N(|\vec{p}|) \equiv \sqrt{\vec{p}^2 + m_N^2} - m_N \quad (30)$$

is the heavy-baryon energy of an on-shell nucleon. The nucleon self-energy  $\Sigma_N(p)$  satisfies  $\Sigma_N(E_N(|\vec{p}|), \vec{p}) = 0$ , and  $Z_N$  is related to  $\Sigma_N(p)$  by

$$Z_N^{-1} = 1 + \left. \frac{\partial}{\partial p_0} \Sigma_N(p) \right|_{p_0=E_N(|\vec{p}|)}. \quad (31)$$

To NNLO,

$$Z_N^{(0)} = 1, \quad (32)$$

$$Z_N^{(1)} = 0, \quad (33)$$

$$Z_N^{(2)} = - \left. \frac{\partial}{\partial p_0} \Sigma_N^{(0)}(p) \right|_{p_0=0}, \quad (34)$$

where  $\Sigma_N^{(0)}$  is the LO nucleon self-energy shown in FIG. 2.

The field renormalization constants are not directly observable. Not surprisingly,  $Z_N^{(2)}$  and  $Z_\pi^{(2)}$  are cutoff-dependent.

## B. $\Delta$ propagator

The loops appearing in the delta self-energy,  $\Sigma_\Delta(p)$ , have both real and imaginary components. The inverse delta propagator is written as

$$S_\Delta^{-1} = p_0 - E_\Delta(|\vec{p}|) + \text{Re}\Sigma_\Delta(p) + \frac{i}{2}\gamma(p) , \quad (35)$$

where

$$E_\Delta(|\vec{p}|) \equiv \sqrt{\vec{p}^2 + m_\Delta^2} - m_N \quad (36)$$

is the heavy-baryon energy of the delta, and

$$\gamma(p) \equiv 2\text{Im}\Sigma_\Delta(p) . \quad (37)$$

We choose to renormalize  $m_\Delta$  so that

$$\text{Re}\Sigma_\Delta(E_\Delta(|\vec{p}|), \vec{p}) = 0 . \quad (38)$$

The regulator dependence that arises in the real part of the self-energy  $\Sigma_\Delta(p)$  at the on-shell point,  $E_\Delta(|\vec{p}|)$ , is thus absorbed in  $\delta$ .

Although the delta need not be an asymptotic state at least in low-energy  $\pi N$  elastic scattering, it is useful to introduce the field renormalization constant  $Z_\Delta$ , which we *define* as

$$Z_\Delta^{-1} \equiv 1 + \frac{\partial}{\partial p_0} [\text{Re}\Sigma_\Delta(p)] \Big|_{p_0=E_\Delta(|\vec{p}|)} . \quad (39)$$

Since the energy dependence of  $\Sigma_\Delta(p)$  only appears at NNLO, the leading few orders of  $Z_\Delta$  are given by

$$Z_\Delta^{(0)} = 1 , \quad (40)$$

$$Z_\Delta^{(1)} = 0 , \quad (41)$$

$$Z_\Delta^{(2)} = -\frac{\partial}{\partial p_0} [\text{Re}\Sigma_\Delta^{(0)}(p)] \Big|_{p_0=\delta} , \quad (42)$$

where  $\Sigma_\Delta^{(0)}$  is the LO delta self-energy given in FIG. 3. We stress that  $Z_\Delta$  is merely an intermediate quantity in our calculation and the definition above is not unique by any means. As we will see in Sec. VB, the amplitude in the end does not depend explicitly on  $Z_\Delta$ .

### C. $\pi N \Delta$ vertex

We *define* the  $\pi N \Delta$  vertex function,  $V_\pi$ , as the sum of all *amputated*  $\Delta \rightarrow \pi N$  subdiagrams that have an incoming delta carrying four-momentum  $(p_0, \vec{p})$  and an outgoing pion with four-momentum  $(k_0, \vec{k})$  and isospin  $a$ . The incoming and outgoing particles are not necessarily on-shell. Rotational and isospin invariance require that  $V_{\pi a}$  be a  $2 \times 4$  matrices in spin and isospin space of the form

$$V_{\pi a} = T_a \left[ \vec{S} \cdot \vec{k} F + \vec{S} \cdot \vec{p} G + \epsilon_{ijl} \Omega_{im} k_j p_l (k_m H + p_m Q) \right], \quad (43)$$

where  $F$ ,  $G$ ,  $H$ , and  $Q$  are three-scalar form factors that depend on  $p_0$ ,  $k_0$ ,  $\vec{p}^2$ ,  $\vec{p} \cdot \vec{k}$ , and  $\vec{k}^2$ . For simplicity, we study only the special case where the incoming delta sits in its own CM frame, *i.e.*,  $\vec{p} = 0$ . The vertex function is simplified as

$$V_{\pi a}^{\text{CM}} = T_a \vec{S} \cdot \vec{k} F(p_0, k_0, k^2), \quad (44)$$

with  $k \equiv |\vec{k}|$ .

The function  $F$  at LO and NLO,  $F^{(0)}$  and  $F^{(1)}$  respectively, is constant and can be read off directly from  $\mathcal{L}^{(0)}$  (14) and  $\mathcal{L}^{(1)}$  (15). At NNLO,  $F^{(2)}(p_0, k_0, k^2)$  consists of  $\nu = 2$  interactions and one-loop diagrams, shown in FIG. 6.  $F^{(2)}(p_0, k_0, k^2)$  has cutoff dependences proportional to  $p_0^2$ ,  $k_0^2$ ,  $p_0 k_0$ ,  $\delta p_0$ ,  $\delta k_0$ ,  $\delta^2$ , and  $m_\pi^2$ . Naively, one could introduce  $\nu = 2$  counterterms that are associated with time derivatives on  $\Delta$  and/or  $\pi$ , in order to absorb divergences associated with  $p_0$  and  $k_0$ . However, those counterterms can always be removed using equations of motion or field redefinitions, that is, they are redundant parameters, which  $S$ -matrix elements do not depend upon. Fortunately, the  $\pi N \Delta$  vertex function need not be cutoff-independent. Since there are other cutoff dependences floating around, such as those in the field renormalization constants and self-energies, what matters is that the combined cutoff dependence cancels out when the ingredients are put together in the EFT amplitude.

As we will see in Sec. V, a cutoff-independent form factor,  $F_R$ , will appear in the amplitude,

$$F_R \equiv \sqrt{Z_\pi} \sqrt{Z_N} \sqrt{Z_\Delta} F(\delta, \omega(k_\delta), k_\delta^2), \quad (45)$$

where  $k_\delta$  is the momentum of the pion when all particles are on-shell,

$$k_\delta = (\delta^2 - m_\pi^2)^{\frac{1}{2}} \frac{[1 + \delta/m_N + (\delta^2 - m_\pi^2)/(2m_N)^2]^{\frac{1}{2}}}{1 + \delta/m_N}. \quad (46)$$

It is worth noting that  $F_R$  is independent of energy by definition. Since the definition of  $Z_\Delta$  is not unique [4], interpreting  $T_a \vec{S} \cdot \vec{k} F_R$  as the CM amplitude for delta decay into  $\pi N$  is questionable.

We stress that  $F_R$  is just another intermediate quantity that will be used later to assemble the  $\pi N$  scattering amplitude.

The LO and NLO of  $F_R$  are the same as those of  $F$ :

$$F_R^{(0)} = F^{(0)} = \frac{h_{A,R}}{2f_\pi}, \quad (47)$$

$$F_R^{(1)} = F^{(1)} = 0. \quad (48)$$

At NNLO, the pion loops bring dependences on  $\delta$  and  $k_\delta$ . To the first approximation,  $\delta = \omega(k_\delta) + \mathcal{O}(k_\delta^2/m_N)$ . In addition,  $F_R^{(2)}$  receives nontrivial one-loop corrections, which are evaluated on-shell by definition, and contributions of the field renormalization constants,

$$F_R^{(2)} = \frac{1}{2} \left( Z_\pi^{(2)} + Z_N^{(2)} + Z_\Delta^{(2)} \right) F^{(0)} + F^{(2)}(\omega(k_\delta), \omega(k_\delta), k_\delta^2) = \frac{h_{A,R}}{2f_\pi} (\varkappa + i\lambda), \quad (49)$$

where

$$\varkappa \equiv \frac{k_\delta^2}{(4\pi f_\pi)^2} \left[ d_R \frac{(4\pi f_\pi)^2 m_\pi^2}{h_{A,R} k_\delta^2} + \text{Re}\mathcal{G}(m_\pi/k_\delta) \right], \quad (50)$$

and

$$\lambda \equiv \frac{k_\delta^2}{(4\pi f_\pi)^2} \text{Im}\mathcal{G}(m_\pi/k_\delta), \quad (51)$$

with

$$\begin{aligned} \mathcal{G}(x) = & \frac{2}{3} (1+x^2)^{-\frac{1}{2}} \left\{ -\pi \left( g_A^2 - \frac{81}{16} g_A^{\Delta^2} \right) x^3 + 2\pi i \left( g_A^2 + \frac{1}{72} h_{A,R}^2 \right) \right. \\ & \left. + \left[ g_A^2 - \frac{1}{72} h_{A,R}^2 (13 + 15x^2) + \frac{81}{16} g_A^{\Delta^2} \right] \ln \left( \frac{\sqrt{1+x^2}-1}{\sqrt{1+x^2}+1} \right) \right\}. \end{aligned} \quad (52)$$

There are two types of divergences arising from the one-loop corrections and field renormalization constants: one is proportional to  $\delta^2$  and the other  $m_\pi^2$ . We can use the bare  $h_A$  to absorb the  $\delta^2$  divergence. In constructing  $\mathcal{L}^{(2)}$  (16), we already used the delta equation of motion to turn the operator  $-(N^\dagger \mathbf{T} \vec{S} \mathcal{D}_0^2 \Delta + H.c.) \cdot \vec{\mathbf{D}}$  into  $\delta^2 (N^\dagger \mathbf{T} \vec{S} \Delta + H.c.)$ , which is subsequently absorbed into the  $h_A$  operator. Therefore, it is appropriate to combine the  $\delta^2$  divergence with the bare  $h_A$ , since there already is a  $\delta^2$  piece in  $h_A$ . A similar argument holds for the  $d$  operator, which is proportional to  $m_\pi^2$  and can be renormalized by the  $m_\pi^2$  divergence. Equations (47), (49), and (50) should be viewed as the definitions of the renormalized coupling constants  $h_{A,R}$  and  $d_R$ . To make expressions compact, we will drop the subscripts “ $R$ ” on  $h_{A,R}$  and  $d_R$  in the rest of this paper.

Note that the logarithm in the function  $\mathcal{G}(x)$  blows up as  $x \rightarrow 0$ , implying that an infrared divergence would arise if one treated  $m_\pi/\delta$  as a higher-order effect, as in the power counting of Ref. [20]. Although this infrared divergence is not a fundamental difficulty, it is convenient to avoid it by considering  $m_\pi \sim \delta$ .

#### D. $\Delta$ self-energy

In this paper we employ the delta rest frame, where the on-shell delta energy is

$$E_{\Delta}(0) = \delta . \quad (53)$$

As we discussed, the delta self-energy produces a large effect only inside the resonance window,  $|E - \delta| = \mathcal{O}(Q^3/M_{\text{QCD}}^2)$ . We will enforce this relation when expanding  $\Sigma_{\Delta}(E)$ . The restriction on the energy domain changes the order-index of  $\Sigma_{\Delta}(E)$ , since the energy dependence of  $\Sigma_{\Delta}(E)$  around  $E = \delta$  is always two powers smaller than  $\Sigma_{\Delta}(\delta)$ , Eq. (19). We denote by  $\widehat{\Sigma}_{\Delta}^{(0)}, \widehat{\Sigma}_{\Delta}^{(1)}, \dots$  the expansion of  $\Sigma_{\Delta}(E)$  within the resonance window.

The diagrams contributing to  $\Sigma_{\Delta}$  at LO, NLO, and NNLO can be found respectively in FIG. 3, FIG. 4, and FIG. 5. Detailed calculations of the delta self-energy can be found in the literature, for example Refs. [13, 39]. Using Eqs. (37), (38), (42), and (20), the three lowest orders of  $\Sigma_{\Delta}(E)$  can then be written as

$$\widehat{\Sigma}_{\Delta}^{(0)}(\delta) = \frac{i}{2}\gamma^{(0)}(\delta) , \quad (54)$$

$$\widehat{\Sigma}_{\Delta}^{(1)}(\delta) = \frac{i}{2}\gamma^{(1)}(\delta) , \quad (55)$$

$$\widehat{\Sigma}_{\Delta}^{(2)}(E) = -\frac{Z_{\Delta}^{(2)}}{S_{\Delta}^{(0)}(E)} + \frac{i}{2}\hat{\gamma}^{(2)}(E) , \quad (56)$$

where

$$\hat{\gamma}^{(2)}(E) \equiv \gamma^{(2)}(\delta) + Z_{\Delta}^{(2)}\gamma^{(0)}(\delta) + (E - \delta)\gamma^{(0)'(\delta)} . \quad (57)$$

Due to the presence of  $Z_{\Delta}^{(2)}, \widehat{\Sigma}_{\Delta}^{(2)}$  is cutoff-dependent. We should appreciate the fact that the energy dependence of  $\text{Re}\Sigma_{\Delta}^{(0)}(E)$  is not present until NNLO, thanks to enforcing  $|E - \delta| = \mathcal{O}(Q^3/M_{\text{QCD}}^2)$ . Had it shown up already in  $\widehat{\Sigma}_{\Delta}^{(0)}$ , an otherwise redundant operator  $i\Delta^{\dagger}\mathcal{D}_0^3\Delta$  would have been necessary in order to absorb the divergence in  $\Sigma_{\Delta}^{(0)}(E)$  that is proportional to  $E^3$ .

The imaginary part of the delta self-energy,  $\gamma(E)$ , can be most conveniently evaluated by cutting the intermediate states that could be on-shell with an injected CM energy  $E$  and then replacing those propagators with the Dirac delta functions that enforce energy-momentum conservation. This is of course equivalent to applying the optical theorem.

In LO and NLO delta self-energy diagrams, the only potentially on-shell intermediate state is a pion and a nucleon. The contribution of such an intermediate state to  $\gamma(E)$  can generally be

written as

$$\begin{aligned}\gamma_{\pi N}(E) &= Z_N Z_\pi \sum_a \int \frac{d^3 l}{(2\pi)^3} \frac{1}{2\omega(l)} V_{\pi a}^{\text{CM}\dagger}(E) V_{\pi a}^{\text{CM}}(E) \times 2\pi\delta(E - E_N(l) - \omega(l)) \\ &= Z_N Z_\pi \mathcal{N}(k) \frac{k^3}{6\pi} |F(E, \omega(k), k^2)|^2,\end{aligned}\quad (58)$$

where, in the last line,  $k$  satisfies

$$E = \omega(k) + E_N(k), \quad (59)$$

and the pre-factor is

$$\mathcal{N}(k) \equiv \frac{E_N(k) + m_N}{E + m_N}. \quad (60)$$

For an on-shell delta, use of Eq. (45) yields

$$\gamma_{\pi N}(\delta) = \mathcal{N}(k_\delta) \frac{k_\delta^3}{6\pi} \frac{|F_R|^2}{Z_\Delta}. \quad (61)$$

Substituting the LO expressions for  $F$  (Eq. (47)),  $Z_\pi$  (Eq. (27)) and  $Z_N$  (Eq. (32)),

$$\gamma^{(0)}(E) = \frac{h_A^2}{24\pi f_\pi^2} \mathcal{N}(k) k^3. \quad (62)$$

Using in  $\mathcal{N}(k_\delta) k_\delta^3$  the exact kinematic relation between  $k_\delta$  and  $\delta$ , Eq. (46),

$$\gamma^{(0)}(\delta) = \frac{h_A^2}{24\pi f_\pi^2} (\delta^2 - m_\pi^2)^{\frac{3}{2}} \left[ 1 + \delta/m_N + (\delta^2 - m_\pi^2)/(2m_N)^2 \right]^{\frac{3}{2}} \frac{1 + \delta/m_N + (\delta^2 - m_\pi^2)/2m_N^2}{(1 + \delta/m_N)^5}, \quad (63)$$

a relation known from isobar models [38]. Analogously, from the NLO expressions for  $F$  (Eq. (48)),  $Z_\pi$  (Eq. (28)), and  $Z_N$  (Eq. (33)),

$$\gamma^{(1)}(\delta) = 0. \quad (64)$$

The strict heavy-baryon expansion of  $\mathcal{N}(k_\delta) k_\delta^3$  gives

$$\gamma^{(0)}(\delta) + \gamma^{(1)}(\delta) + \dots = \frac{h_A^2}{24\pi f_\pi^2} (\delta^2 - m_\pi^2)^{\frac{3}{2}} \left[ 1 - \frac{5\delta}{2m_N} + \frac{42\delta^2 - 7m_\pi^2}{8m_N^2} - \frac{7\delta(22\delta^2 - 7m_\pi^2)}{16m_N^3} + \dots \right]. \quad (65)$$

The first term is the well-known heavy-baryon limit [13]. With  $\delta \sim 300$  MeV, the first, Galilean correction is  $\sim -80\%$  due to the relatively large numerical factor in front of  $\delta/m_N$ . This expansion, nonetheless, still converges as long as  $\delta < m_N$ . More importantly, the slowness of this expansion is not reflected in the EFT expansion of the amplitude. As we will show later, to NLO the  $\pi N$  amplitude only depends on  $\delta$  and  $\gamma^{(0)} + \gamma^{(1)}$ , *i.e.*, it is a simple Breit-Wigner formula. Enforcing



the heavy-baryon expansion in  $\mathcal{N}(k_\delta) k_\delta^3$  does not result in an amplitude with a different functional form, but it does lead to a different value of  $h_A$ . This only means that the value of  $h_A$  depends, because of the slow convergence, on how  $Q/m_N$  corrections are treated. In addition, there are higher-order corrections to  $\gamma$  contributed by the NNLO  $\pi N \Delta$  vertex function, which includes one-loop corrections and an undetermined LEC ( $d$ ). Since there is no *a priori* evidence that these undetermined corrections are smaller than those that are proportional to  $1/m_N^3$  and higher, keeping  $Q/m_N$  terms to all orders does not have any deep significance.

In the following, we consider two cases. In one case, having explained the validity of the heavy-baryon formalism despite the large factor of  $-5\delta/2m_N$ , we carry out the expansion of  $\mathcal{N}(k)k^3$ . We refer to this as the strict heavy-baryon expansion. In the other case, we do not expand  $\mathcal{N}(k)k^3$ , because (i) it is a convenient way to include the required terms up to  $1/m_N^2$ ; (ii) it allows a meaningful comparison of LECs with the literature, where a similar resummation is performed [19, 20]; and (iii) whenever desirable, a strict heavy-baryon expansion in  $Q/m_N$  can easily be worked out. We refer to this second case as the semi-resummation.

When evaluating  $\gamma^{(2)}(\delta)$ , there are a few NNLO delta self-energy diagrams in which an intermediate state of two pions and a nucleon ( $\pi\pi N$ ) could be on-shell if being cut on the middle-nucleon internal line. These diagrams are labeled (a) to (h) in FIG. 5. To estimate the contribution of  $\pi\pi N$  to  $\gamma^{(2)}(\delta)$ , we first notice that the phase space for such an intermediate state to go on-shell is so small that even pions are nonrelativistic, having three-momenta  $\tilde{Q} \sim \sqrt{m_\pi(\delta - 2m_\pi)} \sim 40$  MeV  $\ll m_\pi$ . We can use this fact to refine once again the standard ChPT power counting. To be definite, let us look at the two-loop diagram labeled (a) in FIG. 5. In contrast with the generic situation, we should now replace  $\tilde{Q}$  for  $Q$  where pion three-momenta appear in the loops (vertices, propagators, integrals). Also, the energy of the nucleon is of  $\mathcal{O}(\tilde{Q}^2/m_N)$  rather than  $Q$ . Overall, these changes in the power counting bring a suppression of roughly order  $(\tilde{Q}/m_\pi)^7 \sim 10^{-3} - 10^{-4}$ . This somewhat crude estimate is justified by a phase-shift analysis [28]. The unitarity of the  $S$  matrix suggests that the opening of the  $\Delta \rightarrow \pi\pi N$  channel brings “inelasticities” in  $\pi N$  scattering. However, Ref. [28] gives inelasticities only of order of magnitude  $10^{-3}$  in the delta region. Therefore, though they are formally NNLO, the  $\pi\pi N$  contributions are suppressed by the “accidental” closeness of  $\delta$  to  $2m_\pi$ . Numerically we can thus safely neglect  $\pi\pi N$  contributions,

$$\gamma_{\pi\pi N}(\delta) \simeq 0, \tag{66}$$

and consider only  $\pi N$  contributions.

With this approximation and Eq. (49),  $\gamma^{(2)}(\delta)$  is given by

$$\gamma^{(2)}(\delta) = \left(2\kappa - Z_{\Delta}^{(2)}\right) \gamma^{(0)}(\delta), \quad (67)$$

where  $\kappa$  is given in Eq. (50). Inserting Eq. (67) into Eq. (57) one finds

$$\hat{\gamma}^{(2)}(E) = 2\kappa\gamma^{(0)}(\delta) + \gamma^{(0)'}(\delta)(E - \delta), \quad (68)$$

completing the calculation of the delta self-energy to NNLO.

## V. $\pi N$ SCATTERING AMPLITUDE

In this section we put together the various one- $\Delta$ -irreducible ingredients calculated in the previous section. We first review the kinematics in  $\pi N$  scattering, before constructing the  $T$  matrix in the various channels.

### A. Kinematics

In the CM frame, we denote the initial (final) pion momentum by  $\vec{k}$  ( $\vec{k}'$ ), the initial (final) pion isospin index by  $a$  ( $a'$ ), and the initial (final) nucleon spin  $z$ -component and isospin third-component by  $\sigma$  ( $\sigma'$ ) and  $\tau$  ( $\tau'$ ), respectively. The CM energy, denoted by  $E$ , is given in terms of the pion (nucleon) energy  $\omega(k)$  ( $E_N(k)$ ) by Eq. (59), with  $k \equiv |\vec{k}|$ .

The  $T$  matrix is related to the  $S$  matrix by

$$S = 1 + iT. \quad (69)$$

Asymptotic pion states are normalized so that

$$\langle \pi, \vec{k}' a' | \pi, \vec{k} a \rangle = 2\omega(|\vec{k}|) (2\pi)^3 \delta^{(3)}(\vec{k} - \vec{k}') \delta_{a'a}, \quad (70)$$

while for nucleon states,

$$\langle N, \vec{k}' \sigma' \tau' | N, \vec{k} \sigma \tau \rangle = (2\pi)^3 \delta^{(3)}(\vec{k} - \vec{k}') \delta_{\sigma'\sigma} \delta_{\tau'\tau}. \quad (71)$$

The scattering amplitudes,  $\mathcal{A}_{a'a}$ , are the elements of the  $T$  matrix between the asymptotic pion and nucleon states and can be written as  $2 \times 2$  matrices in nucleon spin and isospin indices,

$$(\mathcal{A}_{a'a})_{\sigma'\sigma, \tau'\tau}(\vec{k}', \vec{k}) \equiv \langle \vec{k}' a' \sigma' \tau' | T | \vec{k} a \sigma \tau \rangle. \quad (72)$$

We normalize the spin-orbital projector  $\mathbb{P}_{jl}$  for a total angular momentum  $j$  and an orbital angular momentum  $l$  so that

$$\int d\Omega_{\hat{k}''} \mathbb{P}_{j'l'}(\hat{k}', \hat{k}'') \mathbb{P}_{jl}(\hat{k}'', \hat{k}) = \delta_{j'j} \delta_{l'l} \mathbb{P}_{jl}(\hat{k}', \hat{k}), \quad (73)$$

with  $d\Omega_{\hat{k}''}$  the area element on a unit three-sphere spanned by  $\hat{k}''$ . The  $\mathbb{P}_{jls}$  with lowest  $js$  and  $ls$  are

$$\mathbb{P}_{\frac{1}{2}0}(\hat{k}', \hat{k}) = \frac{1}{4\pi}, \quad (74)$$

$$\mathbb{P}_{\frac{1}{2}1}(\hat{k}', \hat{k}) = \frac{1}{4\pi} \left[ \hat{k}' \cdot \hat{k} + i \left( \hat{k}' \times \hat{k} \right) \cdot \vec{\sigma} \right], \quad (75)$$

$$\mathbb{P}_{\frac{3}{2}1}(\hat{k}', \hat{k}) = \frac{1}{4\pi} \left[ 2\hat{k}' \cdot \hat{k} - i \left( \hat{k}' \times \hat{k} \right) \cdot \vec{\sigma} \right]. \quad (76)$$

The isospin projector  $\mathbb{I}_t$  for a total isospin  $t$  is normalized so that

$$\sum_c \mathbb{I}_{t'}(a', c) \mathbb{I}_t(c, a) = \delta_{t't} \mathbb{I}_t(a', a). \quad (77)$$

There are only two different  $\mathbb{I}_t$ s in  $\pi N$  scattering:

$$\mathbb{I}_{\frac{1}{2}}(a', a) = \frac{1}{3} (\delta_{a'a} + i\epsilon_{a'ac}\tau_c), \quad (78)$$

$$\mathbb{I}_{\frac{3}{2}}(a', a) = \frac{1}{3} (2\delta_{a'a} - i\epsilon_{a'ac}\tau_c). \quad (79)$$

The normalization factor between the angular-momentum eigenstates and the asymptotic states defined in Eqs. (70) and (71) can be found in many textbooks (see, *e.g.*, Ref. [3]). Without showing the tedious details, we simply state that  $\mathcal{A}_{a'a}$  is related to the phase shifts,  $\theta_{jlt}(E)$ , as follows:

$$i\mathcal{A}_{a'a}(\vec{k}', \vec{k}) \equiv \frac{8\pi^2}{k\mathcal{N}(k)} \sum_{jlt} \mathbb{P}_{jl}(\hat{k}', \hat{k}) \mathbb{I}_t(a', a) \{ \exp[2i\theta_{jlt}(E)] - 1 \}, \quad (80)$$

where  $\mathcal{N}(k)$  is defined in Eq. (60). The partial-wave  $T$ -matrix elements are expressed in terms of  $\theta_{jlt}(E)$  as

$$T_{jlt}(E) \equiv -i \{ \exp[2i\theta_{jlt}(E)] - 1 \}. \quad (81)$$

In the following we will use a more conventional notation for a specific partial wave:  $l_{2t,2j}$ . For example,  $P_{13}$  refers to the  $l = 1$  ( $P$  wave),  $t = 1/2$ , and  $j = 3/2$ .

## B. $T$ matrix

Now we collect all the pieces from Sec. IV to build the  $\pi N$  scattering amplitude in the various waves, Eq. (81). Here the exact relation between  $E$  and  $k$  (Eq. (59)) is assumed, meaning that

certain trivial, kinematic  $k/m_N$  terms are resummed —what we refer to as semi-resummation. In the next section, Sec.V C, we specialize to the strict heavy-baryon expansion.

At LO ( $Q^{-1}$ ) there is only a pole diagram, FIG. 9(A), which contributes only to the  $P_{33}$  wave. From Eqs. (20) and (54),

$$T_{P_{33}}^{\text{LO}} = -\gamma^{(0)}(\delta) S_{\Delta}^{(0)} = -\frac{\gamma^{(0)}(\delta)}{E - \delta + i\gamma^{(0)}(\delta)/2} \left[ 1 + \mathcal{O}\left(\frac{Q}{M_{\text{QCD}}}\right) \right], \quad (82)$$

where  $\gamma^{(0)}(\delta)$  is given by Eq. (63). This is of the form (1) with a resonance at  $E_R = \delta$ , an energy-independent width  $\Gamma = \gamma^{(0)}(\delta)$ , and no background,  $T_B = 0$ . The two independent parameters can be taken to be  $\delta$  and  $h_A$ . This is same result as in any isobar model with the simplest contribution to the width resummed [38].

In next order ( $Q^0$ ), there appear  $Q/m_N$  corrections to the pole diagram, FIG. 9(B), which contribute via corrections to the delta self-energy, Eq. (55). The NLO amplitude has the same form as LO,

$$T_{P_{33}}^{\text{NLO}} = -\frac{\gamma^{(0)}(\delta) + \gamma^{(1)}(\delta)}{E - \delta + i[\gamma^{(0)}(\delta) + \gamma^{(1)}(\delta)]/2} \left[ 1 + \mathcal{O}\left(\frac{Q^2}{M_{\text{QCD}}^2}\right) \right], \quad (83)$$

where  $\gamma^{(1)}(\delta)$  vanishes, as given by Eq. (64), when we do not expand kinematic relations in powers of  $\delta/m_N$ .

The NNLO ( $Q^1$ ) corrections are more complicated. The cutoff dependences in  $V_{\pi}^{(2)}$ ,  $\Sigma_{\Delta}^{(2)}$ ,  $Z_N^{(2)}$ , and  $Z_{\pi}^{(2)}$  make several NNLO pole diagrams (labeled from (1) to (4) in FIG. 9(C)) divergent. The remaining diagrams in FIG. 9(C) involve only  $Q/m_N$  corrections. To see that the divergences of these diagrams in fact cancel each other, consider the sum of these pole diagrams,

$$T_{P_{33}}^{\text{pole}(2)} = -\gamma^{(0)}(\delta) S_{\Delta}^{(0)} \left[ \frac{4f_{\pi}}{h_A} F^{(2)}(\omega(k_{\delta}), \omega(k_{\delta}), k_{\delta}^2) - S_{\Delta}^{(0)} \widehat{\Sigma}_{\Delta}^{(2)}(E) + \frac{\gamma^{(0)'}(\delta)(E - \delta)}{\gamma^{(0)}(\delta)} + Z_N^{(2)} + Z_{\pi}^{(2)} \right]. \quad (84)$$

Using Eqs. (49), (56), and (68), and defining

$$T_B(\delta) \equiv 2\lambda, \quad (85)$$

we find

$$T_{P_{33}}^{\text{pole}(2)} = -\gamma^{(0)}(\delta) S_{\Delta}^{(0)} \left[ -\frac{i}{2} S_{\Delta}^{(0)} \hat{\gamma}^{(2)}(E) + \frac{\hat{\gamma}^{(2)}(E)}{\gamma^{(0)}(\delta)} + iT_B(\delta) \right], \quad (86)$$

where no cutoff dependence is present.

Now summing up all the pole diagrams up to order  $Q^1$ ,

$$\begin{aligned} T_{P_{33}}^{\text{pole}} &= T_{P_{33}}^{\text{LO}} + T_{P_{33}}^{\text{pole}(2)} \\ &= -\gamma^{(0)}(\delta) S_{\Delta}^{(0)} \left[ 1 - \frac{i}{2} S_{\Delta}^{(0)} \hat{\gamma}^{(2)}(E) + \frac{\hat{\gamma}^{(2)}(E)}{\gamma^{(0)}(\delta)} + iT_B(\delta) \right] \left[ 1 + \mathcal{O}\left(\frac{Q^3}{M_{\text{QCD}}^3}\right) \right]. \end{aligned} \quad (87)$$

Within the stated error, we can resum the corrections,

$$T_{P_{33}}^{\text{pole}} = -\frac{\gamma^{(0)}(\delta) + \hat{\gamma}^{(2)}(E)}{E - \delta + i[\gamma^{(0)}(\delta) + \hat{\gamma}^{(2)}(E)]/2} [1 + iT_B(\delta)] \left[ 1 + \mathcal{O}\left(\frac{Q^3}{M_{\text{QCD}}^3}\right) \right]. \quad (88)$$

The result so far relied on an expansion around the resonance, to be joined with a description of the off-pole region. As we discussed in Sec. III C, FIG. 9(D) can be accounted for off-pole by allowing the “full” energy dependence in the external legs in FIG. 9(A). This eventually amounts to replacing in Eq. (88)  $\gamma^{(0)}(\delta)$  with  $\gamma^{(0)}(E)$  and, in addition,  $\hat{\gamma}^{(2)}(E)$  with  $\hat{\gamma}^{(2)}(\delta) = 2\kappa\gamma^{(0)}(\delta)$  in order to avoid over-counting the energy dependence. Moreover, to the order we are working, we can instead replace  $\hat{\gamma}^{(2)}(\delta)$  with  $[(1 + \kappa)^2 - 1]\gamma^{(0)}(E)$ . We then arrive at

$$T_{P_{33}}^{\text{pole/off-pole}} = -\frac{\Gamma(E)}{E - \delta + i\Gamma(E)/2} [1 + iT_B(\delta)] \left[ 1 + \mathcal{O}\left(\frac{Q^3}{M_{\text{QCD}}^3}\right) \right], \quad (89)$$

where, using Eq. (62),

$$\Gamma(E) = \frac{[h_A(1 + \kappa)]^2}{24\pi f_{\pi}^2} k^3 \mathcal{N}(k). \quad (90)$$

Equation (89) resembles Eq. (1) except for the absence of an additional background term  $T_B(\delta)$ , which would sit outside the pole term. The one- $\Delta$ -irreducible trees at order  $Q^1$  will provide the remaining piece expected from unitarity, as we will now show.

In fact, in order to complete order  $Q^1$ , we need to include the remaining trees, FIG. 9(E), which are one- $\Delta$ -irreducible. Their contributions to the  $P_{33}$  channel are found to be

$$T_{P_{33}}^{\text{tree, } 1\Delta} = T_B(E), \quad (91)$$

with

$$T_B(E) = \frac{k^3 \mathcal{N}(k)}{6\pi f_{\pi}^2} \left( \frac{g_A^2}{E} + \frac{1}{36} \frac{h_A^2}{E + \delta} \right). \quad (92)$$

This reduces in leading-order in  $Q/m_N$  to  $T_B(\delta)$  defined in Eq. (85) when  $E = \delta$ , which is exactly the missing piece expected from unitarity. This is certainly not a miracle as EFT is supposed to reproduce the unitarity and analyticity of the  $S$  matrix order by order. However, it does confirm the consistency of our power counting from a particular perspective.

Now one can sum up pole (89) and tree (91) contributions to obtain the  $P_{33}$  partial-wave amplitude. Since the difference between  $E$  and  $\delta$  is higher order in the NNLO pole term (86),

$$T_{P_{33}}^{\text{NNLO}} = -\frac{\Gamma(E)}{E - \delta + i\Gamma(E)/2} [1 + iT_B(E)] + T_B(E) + \mathcal{O}\left(T_{P_{33}}^{\text{LO}} \frac{Q^3}{M_{\text{QCD}}^3}\right). \quad (93)$$

Again we recover a Breit-Wigner form (1), but now with an energy-dependent width, Eq. (90), and an energy-dependent background, Eq. (92). The NNLO amplitude involves four independent parameters,  $\delta$ ,  $h_A$ ,  $g_A$ , and  $\varkappa$ . The EFT thus provides specific energy dependences for  $\Gamma$  and  $T_B$  through the two extra parameters that appear at NNLO,  $g_A$  and  $\varkappa$ . Our amplitude is similar to the one from isobar models [38], except that  $h_A$  in  $\Gamma(E)$  gets corrected by a factor of  $1 + \varkappa$ .

Equation (93) reduces to Eq. (1) with energy-*independent*  $\Gamma(\delta)$  and  $T_B(\delta)$  when  $|E - \delta|$  is small enough. For that to happen, the contribution from  $T_B(\delta)$  must overpower that of the energy dependence of  $\Gamma(E)$ , which according to Eq. (86) requires the size of the energy window to be smaller than the half width. In terms of the scales in the problem, we can define a ‘‘Breit-Wigner window’’  $|E - \delta| \sim \mathcal{O}(Q^4/M_{\text{QCD}}^3)$  where Eq. (1) holds approximately. Outside this small window, the more general form (93) should be used.

Other channels are easy to calculate from the one- $\Delta$ -irreducible tree diagrams in FIG. 9(E). For the remaining  $P$ -wave channels,

$$T_{P_{13}}^{\text{NNLO}} = T_{P_{31}}^{\text{NNLO}} = \frac{1}{4}T_{P_{11}}^{\text{NNLO}} = -\frac{k^3 \mathcal{N}(k)}{12\pi f_\pi^2} \left( \frac{g_A^2}{E} - \frac{2}{9} \frac{h_A^2}{E + \delta} \right) \left[ 1 + \mathcal{O}\left(\frac{Q}{M_{\text{QCD}}}\right) \right]. \quad (94)$$

The one- $\Delta$ -irreducible contributions, Eqs. (92) and (94), are, of course, related to amplitudes found in the literature. They are part of the simplest tree-level delta-isobar model [38], where the relations among the NNLO amplitudes in  $P_{13}$ ,  $P_{31}$ , and  $P_{11}$  were also noticed. These contributions are LO in both deltaless and deltaful EFTs when one uses the standard power counting. Ignoring the delta contribution, namely the terms proportional to  $h_A^2$ , one reproduces the deltaless EFT results in Refs. [9, 10]. Including the delta contribution, our results agree with those in the deltaful EFT given in Refs. [12, 17, 18].

The seagull diagram in FIG. 9(E) (the Weinberg-Tomozawa term) contributes to the  $S_{11}$  and  $S_{31}$  channels. Since the delta does not contribute to these waves, our results reduce to the well-known ChPT expressions at standard LO [3, 6]. In the following, we focus on the  $P$ -waves.

### C. Strict heavy-baryon expansion

We have partially resummed  $Q/m_N$  terms in the amplitudes shown above. More precisely, this semi-resummation consists of keeping the exact kinematic relations (46) between  $\delta$  and  $k_\delta$  in

Eq. (61), and (59) between  $k$  and  $E$  in Eqs. (90), (92), and (94). If, instead, one enforces a strict  $1/m_N$  expansion, there are some small changes in the results.

In the  $P_{33}$  channel, at LO and NLO the amplitude is still given by Eqs. (82) and (83), except that  $\gamma^{(0)}(\delta)$  and  $\gamma^{(1)}(\delta)$  are given by the first two terms in Eq. (65). At NNLO, again the amplitude remains in the same form as Eq. (93) but with different expressions for the width,

$$\Gamma(E) = \frac{[h_A(1 + \varkappa)]^2}{24\pi f_\pi^2} (E^2 - m_\pi^2)^{\frac{3}{2}} \left[ 1 - \frac{5E}{2m_N} + \frac{42E^2 - 7m_\pi^2}{8m_N^2} \right], \quad (95)$$

and for the background,

$$T_B(E) = \frac{(E^2 - m_\pi^2)^{\frac{3}{2}}}{6\pi f_\pi^2} \left( \frac{g_A^2}{E} + \frac{1}{36} \frac{h_A^2}{E + \delta} \right). \quad (96)$$

Like for  $T_B(E)$ , in other  $P$ -waves we simply replace  $k$  with  $\sqrt{E^2 - m_\pi^2}$ :

$$T_{P_{13}}^{\text{NNLO}} = T_{P_{31}}^{\text{NNLO}} = \frac{1}{4} T_{P_{11}}^{\text{NNLO}} = -\frac{(E^2 - m_\pi^2)^{\frac{3}{2}}}{12\pi f_\pi^2} \left( \frac{g_A^2}{E} - \frac{2}{9} \frac{h_A^2}{E + \delta} \right) \left[ 1 + \mathcal{O}\left(\frac{Q}{M_{\text{QCD}}}\right) \right]. \quad (97)$$

The difference between these expressions and the corresponding ones in the previous section is of higher order. Comparing the effects of the two sets of formulas gives a further estimate of the size of higher-order corrections.

#### D. Scattering volumes

Although we do not aim at a precise description of the threshold region, we can extract from our calculation the  $S$ -wave scattering lengths and the  $P$ -wave scattering volumes, which are related to the amplitudes at zero energy.

Up to order  $Q^1$  in the off-pole region, the scattering lengths are, of course, identical to the venerable current-algebra results [3, 8]. The scattering volumes, with the semi-resummation, are

$$a_{P_{33}} = \frac{g_A^2}{12\pi f_\pi^2 m_\pi} \left[ 1 + \left( \frac{\sqrt{2}h_A}{3g_A} \right)^2 \frac{m_\pi/\delta}{1 - m_\pi^2/\delta^2} \left( \frac{5}{4} + m_\pi/\delta \right) \right] (1 + m_\pi/m_N)^{-1}, \quad (98)$$

$$a_{P_{13}} = a_{P_{31}} = \frac{1}{4} a_{P_{11}} = -\frac{g_A^2}{24\pi f_\pi^2 m_\pi} \left[ 1 - \left( \frac{\sqrt{2}h_A}{3g_A} \right)^2 \frac{m_\pi/\delta}{1 + m_\pi/\delta} \right] (1 + m_\pi/m_N)^{-1}. \quad (99)$$

In the strict expansion, the factor of  $(1 + m_\pi/m_N)^{-1}$  should be dropped. The extra suppression  $m_\pi/\delta$  of the delta contributions at threshold is evident, and when  $m_\pi/\delta \rightarrow 0$  the delta decouples, as it should. In the opposite limit,  $m_\pi/\delta \rightarrow \infty$ , the delta contributions grow and the scattering volumes vanish (to order  $Q^1$ ) if  $h_A/g_A = 3/\sqrt{2}$ , as is the case in the large- $N_c$  limit [40]. (Of

course our results do not directly apply to this limit, where the delta and other degrees of freedom are degenerate with the nucleon and do not decay into a nucleon and a pion.) The real world is in-between these two limits: since  $m_\pi/\delta \sim 1/2$  and  $h_A/g_A \sim 3/\sqrt{2}$  (as we are going to see), delta's contributions are neither terribly small nor completely opposite to the nucleon's.

## VI. P-WAVE PHASE SHIFTS

To test our EFT result, we compare it with the phase-shift analysis (PSA) by the George Washington (GW) group [28], which bridges over the delta resonance. With parameters extracted from the fit, we compare the resulting values of the scattering volumes with those obtained by a PSA that focuses on lower energies [29].

We first extract the phase shifts out of the EFT amplitude in such a way that unitarity is preserved perturbatively. For that, we use Eq. (81), expanding both the phase shifts and the  $T$  matrix in powers of  $Q/M_{\text{QCD}}$ : denoting by a superscript  $(n)$  the corresponding power,

$$\exp \left[ 2i \sum_n \theta^{(n)} \right] = 1 + i \sum_n T^{(n)}. \quad (100)$$

Specifically, in the  $P_{33}$  channel at LO,

$$\theta_{P_{33}}^{\text{LO}} = \text{arccot} \left[ 2 \frac{\delta - E}{\gamma^{(0)}(\delta)} \right], \quad (101)$$

at NLO,

$$\theta_{P_{33}}^{\text{NLO}} = \text{arccot} \left[ 2 \frac{\delta - E}{\gamma^{(0)}(\delta) + \gamma^{(1)}(\delta)} \right], \quad (102)$$

and at NNLO,

$$\theta_{P_{33}}^{\text{NNLO}} = \text{arccot} \left[ 2 \frac{\delta - E}{\Gamma(E)} \right] + \frac{T_B(E)}{2}. \quad (103)$$

In the other  $P$  channels,

$$\theta_{P_{13}}^{\text{NNLO}} = \theta_{P_{31}}^{\text{NNLO}} = \frac{1}{4} \theta_{P_{11}}^{\text{NNLO}} = \frac{1}{2} T_{P_{13}}^{\text{NNLO}} = \frac{1}{2} T_{P_{31}}^{\text{NNLO}} = \frac{1}{8} T_{P_{11}}^{\text{NNLO}}. \quad (104)$$

Several LECs enter these EFT results. A number of them can be determined from other processes, such as pion decay. We adopt the following values:  $m_\pi = 139$  MeV,  $m_N = 939$  MeV,  $g_A = 1.29$ , and  $f_\pi = 92.4$  MeV. The value for  $g_A$  is obtained using the Goldberger-Treiman relation,  $g_A = 4\sqrt{\pi} f_\pi f / m_{\pi^+}$ , from the pion-nucleon coupling constant  $f$  determined very precisely in the Nijmegen PSA of two-nucleon data [41]. Note that this includes the chiral-symmetry-breaking



corrections to the pion-nucleon vertex (the Goldberger-Treiman discrepancy), which only appear two orders higher than the highest order we are working at. We have verified that our results are not very sensitive to such small corrections, and that using the chiral-limit value does not affect any of our conclusions. In principle we could determine  $|g_A/f_\pi|$  from our fit, but that would distract from our main objective, the description of the delta resonance. The LECs germane to delta-resonance physics are  $\delta$ ,  $h_A/f_\pi$ , and  $\varkappa$ . These LECs are to be determined from low-energy reactions involving the delta, and we do so here for  $\pi N$  scattering.

Our strategy of fitting is to determine the free parameters,  $\delta$ ,  $h_A$ , and  $\varkappa$  from the  $P_{33}$  phase shifts around the delta peak and then predict the phase shifts at lower energies in all  $P$  waves. As it is clear from Eqs. (101) and (102), the LO and NLO  $P_{33}$  phase shifts have the same functional dependence on  $E$ : LO and NLO only differ by Galilean corrections buried in the width. In the following figures we will display Eqs. (101) and (103) by lines. We fit our curves to the results of the GW PSA [28], which we indicate by dots. The two (four) points around  $\theta_{P_{33}} = \pi/2$  used to determine the two (three) parameters at LO (NNLO) are explicitly marked.

The difference between Eqs. (101) and (103) is itself an estimate of the systematic theoretical error at LO. We estimate the error at NNLO by power counting the higher-order corrections that are neglected. As shown in Eq. (93), the systematic error in the  $P_{33}$  channel is of size  $\mathcal{O}(T_{P_{33}}^{\text{LO}} Q^3/M_{\text{QCD}}^3)$ , while in the other channels it is of  $\mathcal{O}(T_{\text{Non-}\Delta}^{\text{NNLO}} Q/M_{\text{QCD}})$ , see Eq. (94). To make the estimate more concrete, we take for  $M_{\text{QCD}}$  the scale associated with the lowest-lying baryon integrated out in the EFT, the Roper resonance of mass  $m_R = 1440$  MeV. For simplicity we take the factor to be  $m_R - m_N$  in all channels; while this could be a conservative estimate of the error since Roper contributions are likely to be small in channels other than  $P_{11}$ , it might still be representative in the  $P_{33}$  channel, where the next resonance, the  $\Delta(1600)$ , lies above the delta a similar distance. Since  $P$  waves other than  $P_{33}$  are predictions that apply throughout the range of energies we consider,  $Q$  should be given by the pion momentum, so the errors in these channels can be generically estimated as

$$\Delta T_{\text{Non-}\Delta} = \pm T_{\text{Non-}\Delta}^{\text{NNLO}} \frac{k}{m_R - m_N}. \quad (105)$$

In the  $P_{33}$  channel, on the other hand, we take  $Q$  as a measure of the deviation from the resonance, because we would like to make the estimated uncertainty vanish at  $E = \delta$  where we fit to the PSA inputs. We first estimate the errors of  $\Gamma(E)$  and  $T_B(E)$ , then calculate the systematic error of the amplitude using Eq. (93). In doing so the unitarity condition is explicitly preserved. The errors of  $\Gamma(E)$  and  $T_B(E)$  should be proportional to  $E - \delta$ . Near the resonance, where  $\Gamma(E)$  matters,

$E - \delta \sim Q^3/M_{\text{QCD}}^2$ . The third-order correction to  $\Gamma(E)$  is of  $\mathcal{O}(\gamma^{(0)}(\delta) Q^3/M_{\text{QCD}}^3)$ , which then could be estimated by

$$\Delta\Gamma(E) = \pm\Gamma(E)\frac{E - \delta}{m_R - m_N} . \quad (106)$$

The higher-order corrections to  $T_B(E)$  come from one- $\Delta$ -irreducible tree diagrams with one  $\nu = 1$  vertex, and hence are of  $\mathcal{O}(T_B(E) Q/M_{\text{QCD}})$ . Since, like in other channels, these one- $\Delta$ -irreducible diagrams apply throughout the low-energy region,  $E - \delta \sim Q$  and

$$\Delta T_B(E) = \pm T_B(E)\frac{E - \delta}{m_R - m_N} . \quad (107)$$

The systematic-error bands of the NNLO results are shown in the following figures as shaded regions.

The phase shifts for the strict heavy-baryon expansion are shown as dashed line for LO (Eq. (101)) and solid line for NNLO (Eqs. (103) and (104)) in FIGs. 10 and 11.<sup>1</sup> The  $P_{33}$  EFT results agree quite well with the GW PSA past the delta resonance, and then, as expected from a momentum expansion, start to deviate from the data. We see a reasonable convergence pattern, and the small error band helps us understand why the EFT works so well in that channel: there is not much room for the EFT to change at higher orders. The  $P_{13}$  and  $P_{31}$  data are not far from the equality predicted at NNLO, and the  $h_A$  coming out of the  $P_{33}$  fit is such that the EFT curve provides a good description of the average phase shifts, being slightly below the data in the  $P_{13}$  channel and above in  $P_{31}$ . In both cases the empirical phase shifts are within the error bands. In the three channels our fits are comparable to other unitarization methods [24, 25]. Well below the resonance energy, our results are comparable to others at  $\mathcal{O}(Q^1)$  [17, 18], but not as good as  $\mathcal{O}(Q^3)$  [18], which contains further LECs. On the other hand, the discrepancy with data in  $P_{11}$  is out of the error band and thus significant. A similar discrepancy was already seen at LO in Refs. [10, 18], where the focus was energies below the resonance. The discrepancy could be considered a “small” effect compared to the dominant  $P_{33}$  amplitude. Indeed, Refs. [10, 18] found that higher-order corrections improve the EFT description in the  $P_{11}$  channel, allowing a change in the sign of the derivative of the phase shifts at the price of fitting more LECs. Unitarization including the Roper [24, 25] also works well throughout the energy region we consider here.

The LECs extracted from the  $P_{33}$  fit are given in TABLE I, where they are denoted “strict” to emphasize that they were obtained from an amplitude where higher orders in  $Q/m_N$  were not

---

<sup>1</sup> The LO curve in the  $P_{33}$  channel does not vanish at threshold, but, as explained in Sec. III C, the deviation from zero is higher-order compared to the resonance amplitude. Indeed, the  $P_{33}$  phase shift vanishes exactly at threshold starting at NNLO.

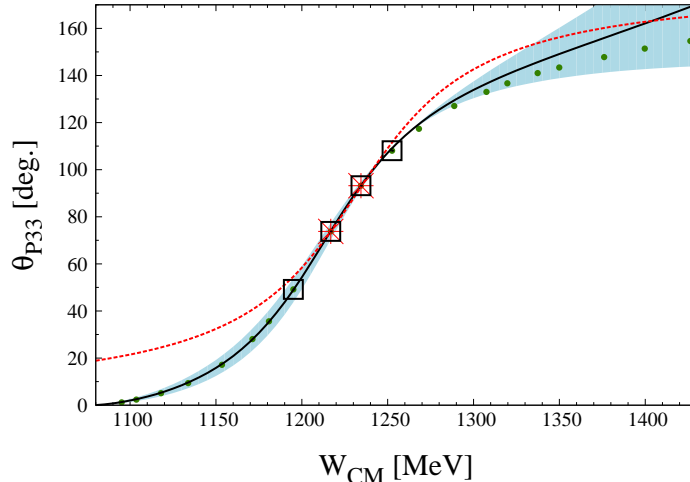


FIG. 10:  $P_{33}$  phase shifts (in degrees) as a function of  $W_{\text{CM}}$  (in MeV), the CM energy including the nucleon mass. The EFT strict heavy-baryon expansion at LO (NNLO) is represented by the red dashed (black solid) line. The NLO curve coincides with LO. The light-blue band outlines the estimated systematic error of the NNLO curve. The green dots are the results of the GW phase-shift analysis [28]. Points marked by a red star (black square) are inputs for LO (NNLO).

TABLE I: Low-energy constants extracted at LO, NLO, and NNLO from the fits using the strict heavy-baryon expansion (strict) and the partial resummation (semi).

	$\delta$ (MeV)			$h_A$			$\varkappa$
	LO	NLO	NNLO	LO	NLO	NNLO	NNLO
strict	293	293	320	1.98	4.21	2.85	0.050
semi	293	293	305	2.71	2.71	2.92	0.058

treated differently than higher orders in  $Q/M_{\text{QCD}}$ . One can estimate the errors in the NNLO values as the variation in each LEC within which the NNLO  $P_{33}$  curve in FIG. 10 roughly stays within the error band. This is of course not a rigorous statistical method; it only serves to indicate how confident we are about the fitted LEC values. This way we find  $\delta/\text{MeV}$ ,  $h_A$ , and  $\varkappa$  to be within  $\sim \pm 4$ ,  $\pm 0.30$ , and  $\pm 0.030$ , respectively, of the NNLO values in TABLE I.

The delta-nucleon mass splitting is related to the position of the delta pole, which can be found by seeking the root of

$$S_{\Delta}^{-1}(E) = E - \delta + i\Gamma(E)/2 = 0. \quad (108)$$

It yields the values given in TABLE II under the label “strict”, which agree fairly well with the values from the GW PSA [28] and from the Review of Particle Physics [1]. In addition to the

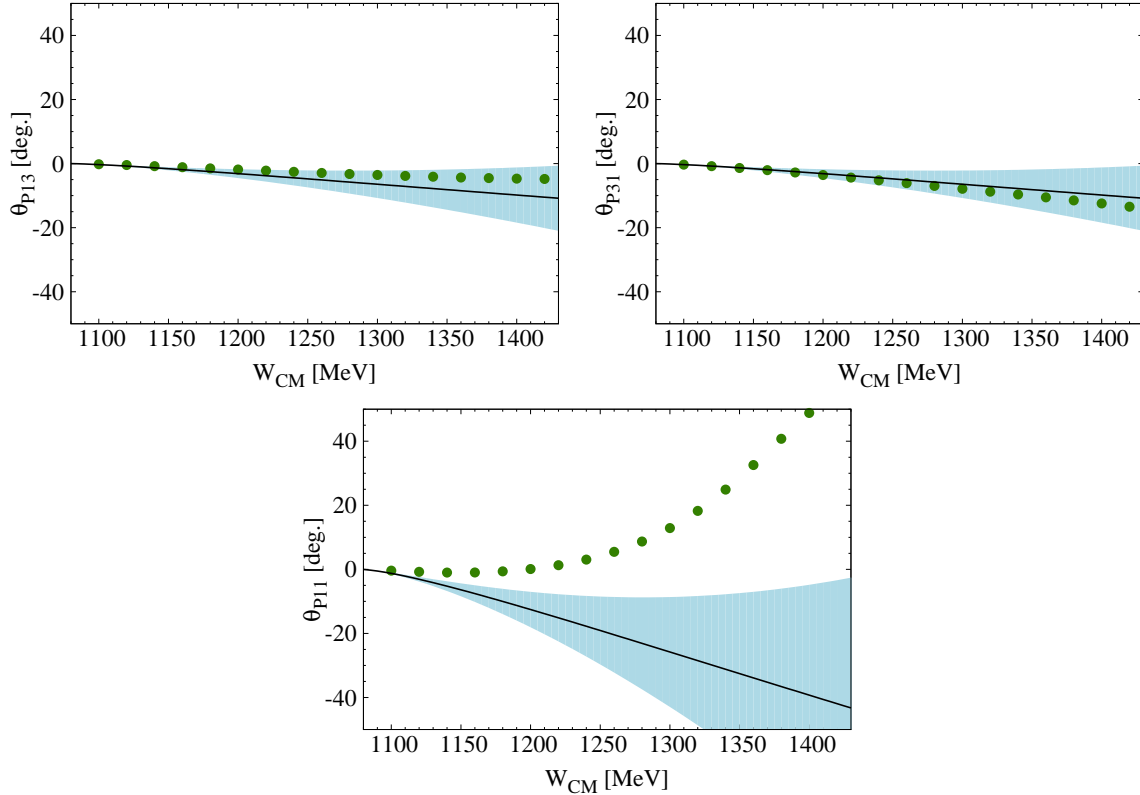


FIG. 11: Predicted phase shifts (in degrees) in the  $P_{13}$ ,  $P_{31}$ , and  $P_{11}$  channels as functions of  $W_{\text{CM}}$  (in MeV), the CM energy including the nucleon mass. LO and NLO vanish in these channels; NNLO EFT results in the strict heavy-baryon expansion are given by the black solid lines. The light-blue bands outline the estimated systematic errors of the NNLO curves. The green dots are the results of the GW phase-shift analysis [28].

value of  $\delta$  in TABLE I, we find at LO  $\Gamma(\delta) = 104$  MeV and at NNLO  $\Gamma(\delta) = 246$  MeV. The Breit-Wigner values [1]  $\delta_{\text{BW}} \approx 1232\text{MeV} - m_N$  and  $\Gamma_{\text{BW}} \approx 118$  MeV are extracted from a fit of the form (1) to data around the resonance peak. Since it is not clear that this window coincides with the “Breit-Wigner window” where our results reduce to Eq. (1), we cannot adopt  $\delta_{\text{BW}}$  and  $\Gamma_{\text{BW}}$  as values for  $\delta$  and  $\Gamma(\delta)$ , even though the pole positions agree. When other reactions are considered within our approach, one should use the value of  $\delta$  determined above. The large value of  $\Gamma(\delta)/2$  at NNLO indicates that it is not a good approximation for the imaginary coordinate of the pole, because the derivatives of  $\Gamma(E)$  in Eq. (108) are not small. Since our NNLO amplitude gives a good fit of the phase shifts, there is nothing intrinsically wrong with our  $\Gamma(E)$ ; what we see here is an example of the general argument given in Ref. [4] that  $\Gamma(\delta)$  is scheme-dependent.

The NNLO value of  $h_A$  we found is consistent with other sources, for example:  $h_A = 1.96 - 2.64$  [18],  $h_A = 2.92$  [19], and  $h_A = 2.81$  [20]. Moreover, we obtain  $h_A/g_A = 2.21$ , close to the large- $N_c$

TABLE II: Pole position of the delta resonance (in MeV) extracted at LO and NNLO from the fits using the strict heavy-baryon expansion (EFT-strict) and the partial resummation (EFT-semi) compared with values from the GW phase-shift analysis (PSA) [28] and the Review of Particle Physics (RPP) [1]. EFT results at NLO are identical to LO.

	LO	NNLO
EFT-strict	$1232 - 52i$	$1211 - 50i$
EFT-semi	$1232 - 52i$	$1211 - 48i$
PSA	$1211 - 49.5i$	
RPP	$\approx 1210 - 50i$	

TABLE III:  $P$ -wave scattering volumes in units of  $m_\pi^{-3}$  (with  $m_\pi$  the charged pion mass): EFT in a strict heavy-baryon expansion (EFT-strict) and with partial resummation of relativistic corrections (EFT-semi) compared with results from a partial-wave analysis (PSA) [29].

	$a_{P_{33}}$	$a_{P_{13}}$	$a_{P_{31}}$	$a_{P_{11}}$
EFT-strict	0.20	-0.034	-0.034	-0.13
EFT-semi	0.18	-0.028	-0.028	-0.11
PSA	0.2100(20)	-0.03159(67)	-0.04176(80)	-0.0799(16)

ratio  $h_A/g_A = 3/\sqrt{2}$  [40]. The third parameter in the fit,  $\varkappa$ , only appears at NNLO, and has several LECs embedded in itself, see Eq. (50):  $d$  and  $g_A^\Delta$ , which have not yet been pinned down at the order we consider here. The central value we obtain is very close to the naive estimate  $(\delta^2 - m_\pi^2)/(4\pi f_\pi)^2 \sim 0.05$ , but from the estimated error we see that  $\varkappa$  is not determined precisely in our fit.

Substituting the fitted values for  $h_A$  and  $\delta$  at NNLO in Eqs. (98) and (99), we find the EFT predictions for  $P$ -wave scattering volumes labeled “strict” in TABLE III. The ratio  $h_A/g_A$  overcompensates for the  $m_\pi/\delta$  suppression, so that the delta contributions are not negligible. The EFT predictions are compared to the values extracted from the low-energy PSA of Ref. [29], which are consistent with earlier extractions. We see good agreement for  $P_{33}$  and  $P_{13}$ , and  $P_{31}$  is not too far off. The 1/4 ratio between  $P_{11}$  and  $P_{31}$ , predicted in Eq. (99), is not respected well in the real world. This is a reflection of the discrepancy between the EFT prediction and the GW PSA in the  $P_{11}$  channel shown in FIG. 11.

As we see, the EFT in the strict heavy-baryon expansion works pretty well for observables (except for  $P_{11}$ ), showing in the first two nontrivial orders good convergence to the data. However, there are also hints that the convergence is slow when one looks at how the parameters, particularly

$h_A$ , change with order in TABLE I. It is also a bit surprising, but not necessarily significant, that  $\Gamma(\delta)$  is found at NNLO to be much larger than  $\Gamma_{\text{BW}}$ .

The strict heavy-baryon expansion is in powers of  $Q/M_{\text{QCD}}$  and  $\delta/M_{\text{QCD}}$ , and when  $Q \sim \delta$  neither is a particularly small ratio. One can get a sense for the size of the corrections by considering the case where we retain some of the relativistic  $Q/m_N$  and  $\delta/m_N$  corrections to all orders, the approach we call semi-resummation. We have already discussed in Sec. IV D how the slow convergence of the  $\delta/m_N$  expansion affects the width. We now turn to its effects in comparison to data.

At LO and NLO in the semi-resummation, there is no change in phase shifts compared to the strict heavy-baryon expansion, and therefore also no change in the position of the delta pole; only the relationship between width and parameters changes, and thus the parameters come out different. At NNLO, the  $P_{33}$  phase shifts, and with them the pole position, change because the dependence of the width on the energy is slightly modified. In FIG. 12, we compare the NNLO results (Eqs. (103) and (104)) of the partial resummation of relativistic corrections with those of the strict heavy-baryon expansion, exhibited before in FIGS. 10 and 11. The semi-resummation fit parameters, delta pole position, and scattering volumes are labeled “semi” in TABLES I, II, and III, respectively. In this case we estimate the errors in  $\delta/\text{MeV}$ ,  $h_A$ , and  $\varkappa$  to be within  $\sim \pm 3$ ,  $\pm 0.20$ , and  $\pm 0.02$ , respectively, of the values in TABLE I. At NNLO  $\Gamma(\delta) = 155 \text{ MeV}$ .

There is a slight improvement in the  $P_{33}$  phase shifts above the resonance, and the width at resonance is closer to the Breit-Wigner value, without destroying the good fit at lower energies. The fitted parameters vary less with order than in the strict expansion, but at NNLO parameters in two schemes agree within 5%, except for the small parameter  $\varkappa$ , where they differ by  $\simeq 15\%$ . The  $P_{13}$  phases move in the right direction for most energies. In the other channels, the situation is less positive. The  $P_{31}$  phases get significantly worse. Finally, there is improvement in the  $P_{11}$  channel, but sizable higher-order contributions are still needed to get anywhere close to the empirical phase shifts.

There are thus regions where each approach gets a better fit to data than the other. It is important to note that the semi-resummed curves are more or less within the error bands of their strict heavy-baryon counterparts, as one would expect from the fact that the differences between two methods are higher-order effects. Overall, we do not find that either the semi-resummation or the strict heavy-baryon works considerably better in describing data than the other.

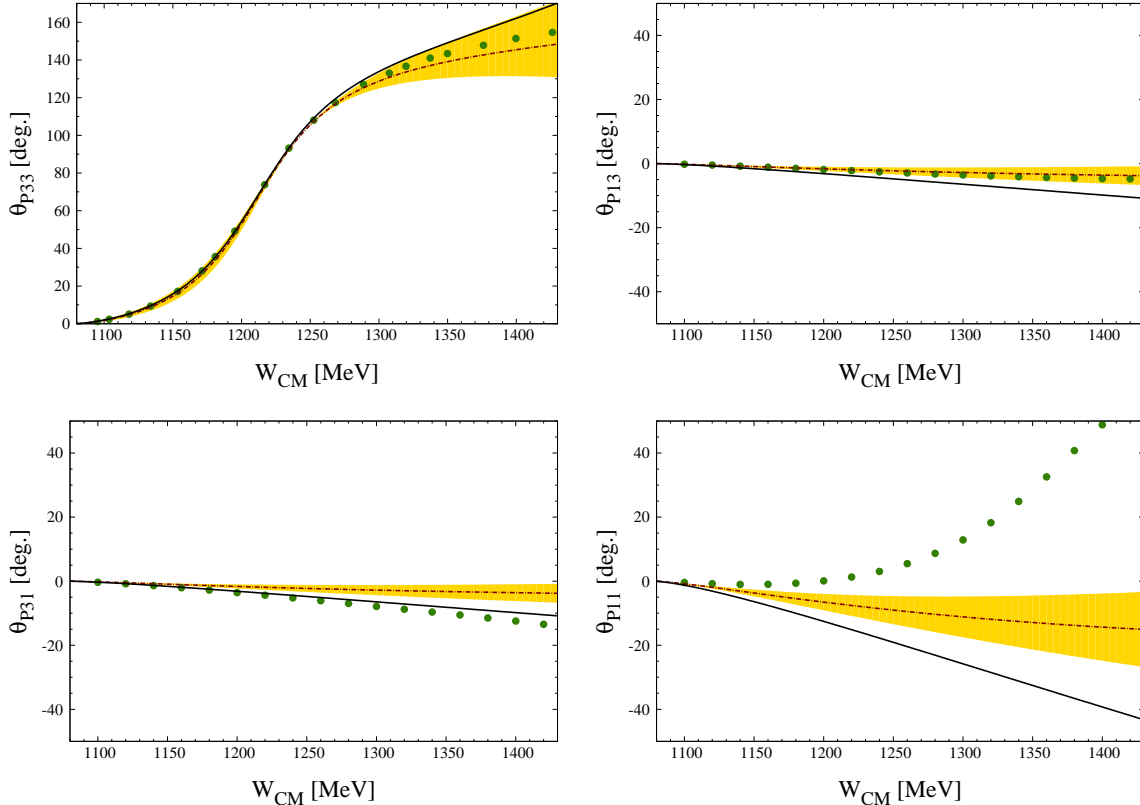


FIG. 12: Comparison of NNLO  $P$ -wave phase shifts (in degrees) as functions of  $W_{\text{CM}}$  (in MeV), the CM energy including the nucleon mass. The black solid (maroon dot-dashed) lines are the strict heavy-baryon (semi-resummed) results. The golden bands outline the estimated systematic errors of the semi-resummed expansion. The green dots are the results of the GW phase-shift analysis [28].

## VII. SUMMARY AND CONCLUSION

We have shown, using  $\pi N$  scattering as an example, how to generalize standard ChPT so that one can cope with the non-perturbative delta resonance within EFT. Our method is similar in spirit to that developed in Refs. [20–22], but differs in detail. It can be thought of as a partial supporting argument for previous, successful unitarization results [24, 25].

ChPT has been generalized to include an explicit field for the delta isobar. We built on earlier work [13, 15] based on the heavy-baryon formalism, which treats the delta as a nonrelativistic particle from the very beginning, rather than relying on a relativistic Lagrangian of the Rarita-Schwinger field. We worked out the  $\mathcal{O}(Q^2/m_N^2)$  relativistic corrections to the  $\pi N \Delta$  vertex within this approach.

EFTs are based on expansions in powers of the ratio of low to high scales,  $M_{\text{lo}}/M_{\text{hi}}$ . The rationale to include the delta as an explicit degree of freedom is that an expansion makes sense

when  $M_{\text{lo}} \sim m_\pi \sim \delta$  and  $M_{\text{hi}} \sim M_{\text{QCD}}$ . Such an expansion is straightforward away from regions of phase space where the delta goes on shell [13–15], but it requires change otherwise: certain contributions are enhanced when the external energy is dialed to the delta-nucleon mass difference. A way to deal with these enhancements had been explored in Refs. [20–22], in which  $m_\pi$  and  $\delta$  were considered separate scales. Here we followed a similar approach to nuclear resonances [26] and constructed a power counting that incorporates the kinematic fine-tuning at the delta pole while keeping  $M_{\text{lo}} \sim m_\pi \sim \delta$ . Our approach resulted in a global EFT description for both the threshold and resonance regions.

Like other EFTs that deal with non-perturbative phenomena, ours captures the non-perturbative structure in LO. Subsequently, the power counting leads to a systematic, perturbative improvement beyond LO. We applied this power counting to low-energy  $\pi N$  scattering, where we built the amplitudes up to NNLO. We have considered both a strict heavy-baryon expansion and a partial resummation of relativistic effects, which yielded comparable results.

Up to NNLO, we could cast our  $P_{33}$  amplitude in terms of a Breit-Wigner form with energy-dependent width and background. Our EFT result is, however, not a mere reproduction of Eq. (1): with our approach, (1) the size of the background can be estimated beforehand; (2) one need not “cautiously” choose the proper energy domain for the resonance window; and (3) there is a link between the energy dependences in the width and background via the parameters  $\delta$ ,  $h_A$ , and  $\varkappa$ , which are then constrained by both the threshold and resonance data.

We fitted our  $P$ -wave amplitudes to the phase shifts given by Ref. [28]. With just three free parameters, we obtained a good fit in the  $P_{33}$  channel. Contrary to an *ad hoc* resummation in the resonance region [19], we had no difficulty preserving the unitarity condition around the resonance. We found parameters consistent with other determinations. With them, the  $P_{13}$  and  $P_{31}$  channels come out qualitatively correct. In the  $P_{11}$  channel a sizable discrepancy exists between the EFT prediction, which is repulsive, and the empirical phase shifts, which become attractive within the region of study.

In order to improve the description of the  $\pi N$  data it is imperative to include other effects. One can push the calculation to next order ( $\mathcal{O}(Q^2)$ ), when in channels other than  $P_{33}$  our framework should yield results similar to Ref. [18]. These lead to a better description of the phases, at least near threshold, and in particular were found to alleviate the  $P_{11}$  discrepancy. The lack of attraction in this channel has been noticed long ago in the context of models, and it has been attributed to the Roper resonance’s fairly large width (see, *e.g.*, Ref. [38]). At  $\mathcal{O}(Q^2)$  Roper effects can appear through low-energy constants. Alternatively, Ref. [17] made an attempt of incorporating an explicit



Roper field in EFT but only investigated the region that is below the delta resonance. One can use the framework presented here to improve the description of the  $P_{11}$  channel up to the energy of the Roper resonance.

We have thus extended ChPT in  $\pi N$  scattering to the delta region. The EFT approach presented in this paper also provides the basis for a model-independent, unified description, from threshold to past the delta resonance without discontinuity, of reactions involving other probes and targets, including nuclei. These reactions, some of which have already been successfully studied with the pioneering power counting of Ref. [20], present further tests of our power counting. A comprehensive confrontation of results from the two approaches should indicate which one provides a more efficient organization of EFT interactions.

### Acknowledgments

We thank Daniel Phillips, Vladimir Pascalutsa, James Friar, and (at a very early stage) Nadia Fettes for useful discussions. Comments on the manuscript by Daniel Phillips were greatly appreciated. We are grateful to the following institutions for hospitality during the long gestation of this work: Los Alamos National Laboratory (BwL), the Kernfysisch Versneller Instituut at Rijksuniversiteit Groningen (UvK), the National Institute for Nuclear Theory at the University of Washington (BwL, UvK), and the University of Arizona (BwL). This work was supported by the US DOE (BwL, UvK) and the Alfred P. Sloan Foundation (UvK).

### Appendix: Slow-velocity boosts

A “heavy” particle is one that has three-momentum  $Q \ll m$ , with  $m$  the mass of the particle. What we are looking for here is a Lorentz transformation rule for a heavy-particle field that is expressed in a perturbative fashion in powers of  $Q/m \ll 1$ . For  $Q/m$  to remain small, boosts of the frame under consideration have to be in small velocities  $\sim Q/m$ . What we are studying here is in fact a special case of the heavy-baryon formalism, in which the four-velocity label  $v = (1, \vec{0})$ . Since  $v = (1, \vec{0})$  is sufficient for all the processes considered in this paper, we are not concerned with the invariance of the Lagrangian under a variation of  $v$ , namely, reparameterization invariance [42]. More details will appear in Ref. [32].

A Poincaré transformation takes a spacetime point  $x^\mu$  to

$$x'^\mu = \Lambda^\mu_\nu x^\nu + a^\mu, \quad (\text{A.1})$$

with  $a^\mu$  a four-vector representing the spacetime translation and  $\Lambda_{\nu'}^\mu$  the Lorentz-transformation matrix. The Poincaré group has ten generators: the time translation  $H$ , spatial translations  $\vec{P}$ , spatial rotations  $\vec{J}$ , and boosts  $\vec{K}$ . The commutation relations among these generators, or the Poincaré algebra, can be readily found in the literature. We adopt the notation used in Ref. [33]. The most commonly used Poincaré representations are a class of fields  $\Phi_l(x)$ , with  $l$  a discrete index, that transform under the Poincaré group as

$$\Phi_{l'}(x) = M(\Lambda)_{l'l} \Phi_l(x'') , \quad (\text{A.2})$$

where  $M(\Lambda)$  is a finite-dimension spacetime-independent matrix that furnishes a representation of the homogeneous Lorentz group and

$$x'' \equiv \Lambda^{-1}(x - a) . \quad (\text{A.3})$$

Therefore, for any (non-unitary) finite-dimension representation of the homogeneous Lorentz group, a corresponding Poincaré representation can be constructed using Eq. (A.2). Such representations include the well-known Klein-Gordon scalar field, Dirac field, four-vector field, *etc.*

However, the Foldy-Wouthuysen (FW) representation [33] does not fall in the above category. A (classical) FW field with mass  $m$  and spin  $s$ ,  $\chi(t, \vec{x})$ , is an  $SO(3)$   $(2s + 1)$ -component spinor. The spin operators,  $\vec{s}$ , are three  $(2s + 1) \times (2s + 1)$  matrices, satisfying

$$[s_i, s_j] = i\epsilon_{ijk} s_k . \quad (\text{A.4})$$

The FW representation is furnished by identifying  $H$ ,  $\vec{P}$ ,  $\vec{J}$ , and  $\vec{K}$  as follows,

$$H = \omega , \quad (\text{A.5})$$

$$\vec{P} = \vec{p} , \quad (\text{A.6})$$

$$\vec{J} = \vec{x} \times \vec{p} + \vec{s} , \quad (\text{A.7})$$

$$\vec{K} = \frac{1}{2} (\vec{x}\omega + \omega\vec{x}) - \frac{\vec{s} \times \vec{p}}{m + \omega} - t\vec{p} , \quad (\text{A.8})$$

with  $\vec{p} \equiv -i\vec{\nabla}$  and  $\omega \equiv (m^2 + \vec{p}^2)^{\frac{1}{2}}$ . One can check that the above definition does satisfy the Poincaré algebra. In particular, an infinitesimal boost can be written as

$$\chi'(t, \vec{x}) \equiv (1 - i\vec{\xi} \cdot \vec{K})\chi(t, \vec{x}) , \quad (\text{A.9})$$

where the boost is parameterized by  $\vec{\xi}$ , which is sometimes referred to as rapidity and is related to the relative velocity  $\vec{V}$  between the original and boosted frame through

$$\vec{\xi} = \hat{V} \tanh^{-1} V . \quad (\text{A.10})$$

Because  $\omega$  is a non-local operator, the FW representation is not as useful in relativistic situations as the Dirac field and the like. But the formal expansion of  $\omega$  and  $\vec{K}$  in powers of  $|\vec{p}|/m$  enables one to derive a perturbative Lorentz transformation rule for the FW field,

$$\omega = m + \frac{\vec{p}^2}{2m} - \frac{\vec{p}^4}{8m^3} + \dots, \quad (\text{A.11})$$

$$\vec{K} = m\vec{x} - t\vec{p} + \frac{1}{4m} (\vec{p}^2\vec{x} + \vec{x}\vec{p}^2) - \frac{1}{2m}\vec{s} \times \vec{p} + \dots. \quad (\text{A.12})$$

We *define* the LO Lorentz transformation so as to reproduce the Galilean transformation. We take  $|\vec{p}| \sim Q$ , so that the kinetic energy  $E \equiv \omega - m$  scales as  $\sim Q^2/m$ . Using the uncertainty principle, we expect that  $|\vec{x}| \sim 1/Q$  and  $t \sim 1/E \sim m/Q^2$ . Also, we power count  $\vec{s}$  as  $|\vec{s}| \sim 1$ . Therefore, the LO boost generators are

$$\vec{K}^{(0)} = m\vec{x} - t\vec{p}, \quad (\text{A.13})$$

and  $\xi \sim Q/m$ . It is worth noting that  $\vec{K}^{(0)}$  does not depend on the spin operator, as indeed it should not.

To remove the inert rest energy  $m$ , we define the heavy field

$$\Psi(t, \vec{x}) \equiv e^{imt} \chi(t, \vec{x}), \quad (\text{A.14})$$

for which

$$i\partial_t \Psi(t, \vec{x}) = (\omega - m)\Psi(t, \vec{x}). \quad (\text{A.15})$$

An infinitesimal Galilean transformation of  $\Psi(t, \vec{x})$  is found to be

$$\Psi'(t, \vec{x}) = \left(1 - im\vec{\xi} \cdot \vec{x} + t\vec{\xi} \cdot \vec{\nabla}\right) \Psi(t, \vec{x}) = \left\{ \left[1 - im\vec{\xi} \cdot \vec{x} + \mathcal{O}(Q/m)\right] \Psi \right\} (t'', \vec{x}''), \quad (\text{A.16})$$

where

$$t'' = (\Lambda^{-1}x)_0 = t + \vec{\xi} \cdot \vec{x}, \quad (\text{A.17})$$

$$x''_i = (\Lambda^{-1}x)^i = x_i + t\xi_i. \quad (\text{A.18})$$

For simplicity, we denote the boost transformation by

$$\Psi \rightarrow \left[1 - im\vec{\xi} \cdot \vec{x}\right] \Psi, \quad (\text{A.19})$$

with the understanding that the left-hand side is evaluated at  $(t, \vec{x})$  while the right-hand side at  $(t'', \vec{x}'')$ .

Going further down in the expansion in Eq. (A.12), one finds the NLO boost generators,

$$\vec{K}^{(1)} = \frac{1}{4m} (\vec{p}^2 \vec{x} + \vec{x} \vec{p}^2) - \frac{1}{2m} \vec{s} \times \vec{p}, \quad (\text{A.20})$$

which depend on spin. The transformation rule for the nucleon field is worked out with  $\vec{s} = \vec{\sigma}/2$ ,

$$N \rightarrow \left[ 1 - im_N \vec{\xi} \cdot \vec{x} + \frac{i}{2m_N} \vec{\xi} \cdot \vec{\nabla} + \frac{1}{4m_N} \vec{\xi} \cdot (\vec{\sigma} \times \vec{\nabla}) + \mathcal{O}(Q^3/m_N^3) \right] N. \quad (\text{A.21})$$

When dealing with the delta, one needs to keep in mind that the mass-splitting  $\delta \sim Q$  in addition to the fact that the delta has spin 3/2,

$$\Delta \rightarrow \left[ 1 - im_N \vec{\xi} \cdot \vec{x} + \frac{i}{2m_N} \vec{\xi} \cdot \vec{\nabla} + \frac{1}{2m_N} \vec{\xi} \cdot (\vec{S}^{(3/2)} \times \vec{\nabla}) + \mathcal{O}(Q^3/m_N^3) \right] \Delta. \quad (\text{A.22})$$

Although  $\delta$  does not appear in the boost at this order, it does show up in the expansion of the kinetic energy.

Our basic strategy to build an order-by-order Lorentz-invariant Lagrangian is the following: (i) enumerate all the rotationally invariant operators according to a certain scheme, *e.g.*, the chiral index  $\nu$  defined in Eq. (13); (ii) use Eqs. (A.21) and (A.22) to constrain the coefficients of these operators so as to preserve Lorentz invariance up to the order under consideration. Up to index  $\nu = 2$  we find the terms shown in Eqs. (14), (15), and (16). One can explicitly check that the  $\pi N \Delta$  operators, for example, are Lorentz invariant in the sense that Lorentz-violating effects only arise at  $\nu = 3$  or higher.

- 
- [1] C. Amsler *et al.* (Particle Data Group), *Phys. Lett.* **B667** (2008) 1.
  - [2] M.L. Goldberger and K.M. Watson, *Collision Theory*, John Wiley & Sons, Inc., New York (1964).
  - [3] S. Weinberg, *Quantum Theory of Fields*, Vol. 2, Cambridge University Press, New York (1996).
  - [4] D. Djukanovic, J. Gegelia, and S. Scherer, *Phys. Rev.* **D76** (2007) 037501.
  - [5] S. Weinberg, *Physica* **96A** (1979) 327; J. Gasser and H. Leutwyler, *Ann. Phys.* **158** (1984) 142; *Nucl. Phys.* **B250** (1985) 465.
  - [6] V. Bernard, N. Kaiser, and U.-G. Meißner, *Int. J. Mod. Phys.* **E4** (1995) 193; V. Bernard, *Prog. Part. Nucl. Phys.* **60** (2008) 82.
  - [7] U. van Kolck, *Prog. Part. Nucl. Phys.* **43** (1999) 337; E. Epelbaum, *Prog. Part. Nucl. Phys.* **57** (2006) 654.
  - [8] S. Weinberg, *Phys. Rev. Lett.* **17** (1966) 616; Y. Tomozawa, *Nuovo Cim.* **46A** (1966) 707.
  - [9] M. Mojžiš, *Eur. Phys. J.* **C2** (1998) 181.
  - [10] N. Fettes, U.-G. Meißner, and S. Steininger, *Nucl. Phys.* **A640** (1998) 199; N. Fettes and U.-G. Meißner, *Nucl. Phys.* **A676** (2000) 311; *Nucl. Phys.* **A693** (2001) 693.

- [11] T. Becher and H. Leutwyler, *JHEP* **0106** (2001) 017.
- [12] V.R. Pandharipande, D.R. Phillips, and U. van Kolck, *Phys. Rev.* **C71** (2005) 064002.
- [13] E. Jenkins and A.V. Manohar, *Phys. Lett.* **B259** (1991) 353; in *Effective Field Theories of the Standard Model*, U.-G. Meißner (editor), World Scientific, Singapore (1992); E. Jenkins, *Nucl. Phys.* **B375** (1992) 561.
- [14] T.R. Hemmert, B.R. Holstein, and J. Kambor, *Phys. Lett.* **B395** (1997) 89; *J. Phys.* **G24** (1998) 1831.
- [15] U. van Kolck, Ph.D dissertation, U. of Texas (1993); C. Ordóñez, L. Ray, and U. van Kolck, *Phys. Rev. Lett.* **72** (1994) 1982; *Phys. Rev.* **C53** (1996) 2086; U. van Kolck, *Phys. Rev.* **C49** (1994) 2932; T.D. Cohen, J.L. Friar, G.A. Miller, and U. van Kolck, *Phys. Rev.* **C53** (1996) 2661.
- [16] N. Kaiser, S. Garstendörfer, and W. Weise, *Nucl. Phys.* **A637** (1998) 395; H. Krebs, E. Epelbaum, and U.-G. Meißner, *Eur. Phys. J.* **A32** (2007) 127.
- [17] A. Datta and S. Pakvasa, *Phys. Rev.* **D56** (1997) 4322.
- [18] N. Fettes and U.-G. Meißner, *Nucl. Phys.* **A679** (2001) 629.
- [19] P.J. Ellis and H.-B. Tang, *Phys. Rev.* **C57** (1998) 3356; K. Torikoshi and P.J. Ellis, *Phys. Rev.* **C67** (2003) 015208.
- [20] V. Pascalutsa and D.R. Phillips, *Phys. Rev.* **C67** (2003) 055202; V. Pascalutsa, *Prog. Part. Nucl. Phys.* **61** (2008) 27.
- [21] V. Pascalutsa and M. Vanderhaeghen, *Phys. Rev. Lett.* **94** (2005) 102003; *Phys. Rev. Lett.* **95** (2005) 232001; *Phys. Rev.* **D73** (2006) 034003; *Phys. Rev.* **D77** (2008) 014027.
- [22] V. Pascalutsa, M. Vanderhaeghen, and S.N. Yang, *Phys. Rept.* **437** (2007) 125.
- [23] S. Weinberg, *Phys. Lett.* **B251** (1990) 288; *Nucl. Phys.* **B363** (1991) 3.
- [24] U.-G. Meißner and J.A. Oller, *Nucl. Phys.* **A673** (2000) 311.
- [25] M.F.M. Lutz and E.E. Kolomeitsev, *Nucl. Phys.* **A700** (2002) 193.
- [26] P.F. Bedaque, H.W. Hammer, and U. van Kolck, *Phys. Lett.* **B569** (2003) 159.
- [27] C.A. Bertulani, H.W. Hammer, and U. van Kolck, *Nucl. Phys.* **A712** (2002) 37.
- [28] R.A. Arndt, W.J. Briscoe, I.I. Strakovsky, and R.L. Workman, *Phys. Rev.* **C74** (2006) 045205; R.A. Arndt, W.J. Briscoe, I.I. Strakovsky, R.L. Workman, and M.M. Pavan, *Phys. Rev.* **C69** (2004) 035213; R.A. Arndt *et al.*, The SAID program, <http://gwdac.phys.gwu.edu/>.
- [29] E. Matsinos, W.S. Woolcock, G.C. Oades, G. Rasche, and A. Gashi, *Nucl. Phys.* **A778** (2006) 95.
- [30] V. Bernard, N. Kaiser, J. Kambor, and U.-G. Meißner, *Nucl. Phys.* **B388** (1992) 315.
- [31] J.J. Sakurai, *Modern Quantum Mechanics*, Addison-Wesley, USA (1994).
- [32] Bingwei Long, in preparation.
- [33] L.L. Foldy and S.A. Wouthuysen, *Phys. Rev.* **78** (1950) 29; L.L. Foldy, *Phys. Rev.* **102** (1956) 568.
- [34] S. Weinberg, *Phys. Rev.* **166** (1968) 1568.
- [35] S. Coleman, J. Wess, and B. Zumino, *Phys. Rev.* **177** (1969) 2239; C.G. Callan, S. Coleman, J. Wess, and B. Zumino, *Phys. Rev.* **177** (1969) 2247.
- [36] E. Jenkins, *Phys. Rev.* **D53** (1996) 2625.

- [37] S.R. Beane and M.J. Savage, *Nucl. Phys.* **A717** (2003) 104.
- [38] T. Ericson and W. Weise, *Pions and Nuclei*, Clarendon Press, Oxford (1988).
- [39] M.K. Banerjee and J. Milana, *Phys. Rev.* **D52** (1995) 6451; C. Hacker, N. Wies, J. Gegelia, and S. Scherer, *Phys. Rev.* **C72** (2005) 055203; A. Semke and M.F.M. Lutz, *Nucl. Phys.* **A778** (2006) 153.
- [40] A. Manohar, hep-ph/9802419.
- [41] U. van Kolck, M.C.M. Rentmeester, J.L. Friar, T. Goldman, and J.J. de Swart, *Phys. Rev. Lett.* **80** (1998) 4386; J.J. de Swart, M.C.M. Rentmeester, and R.G.E. Timmermans, *PiN Newslett.* **13** (1997) 96; U. van Kolck, J.L. Friar, and T. Goldman, *Phys. Lett.* **B371** (1996) 169.
- [42] M.E. Luke and A.V. Manohar, *Phys. Lett.* **B286** (1992) 348.